FINAL REPORT

ON

NGR-17-003-018

THE TRANSMISSION OF SOUND IN NONUNIFORM DUCTS

BY

WALTER EVERSMAN

SUBMITTED TO

NASA-LEWIS RESEARCH CENTER

BY

WICHITA STATE UNIVERSITY

Abstract

The method of weighted residuals in the form of a modified Galerkin method with boundary residuals is developed for the study of the transmission of sound in nonuniform ducts carrying a steady, compressible flow. In this development the steady flow is modeled as essentially one dimensional but with a kinematic modification to force tangency of the flow at the duct walls. Three forms of the computational scheme are developed using for basis functions (a) the no-flow uniform duct modes, (b) positive running uniform duct modes, with flow, and (c) positive and negative running uniform duct modes, with flow. The formulation using the no-flow modes is the most highly developed and has advantages primarily due to relative computational simplicity. Results using the three methods are shown to converge to known solutions for several special cases. The most significant check case is against low frequency, one dimensional results over the complete subsonic Mach number range. Development of the method is continuing, with emphasis on assessing the relative accuracy and efficiency of the three implementations.

INTRODUCTION

The method of weighted residuals (MWR) in the form of a Galerkin technique with boundary residuals, has been shown to be a useful method for the investigation of the transmission of sound in nonuniform ducts with no flow[1]. In this paper the method is extended to treat the case when the duct carries a steady nonuniform flow.

The introduction of steady mean flow into the study of nonuniform duct propagation complicates the problem in two ways. The acoustic field equations no longer reduce to either the simple wave equation of the noflow case or the convective wave equation of the uniform flow case. In addition, the field equations represent acoustic perturbations on a steady nonuniform flow field which in itself is difficult to describe. As a consequence of these complications, no simple theories of propagation have been developed and investigations appearing in the literature have been relatively few.

The majority of studies appearing have been based on a one dimensional theory which treats the propagation as plane waves moving in a one dimensional nozzle flow. Powell[2], Eisenberg and Kao[3] King and Karamcheti[4], Huerre and Karamcheti[5] and Davis[6] have studied one dimensional models by a variety of techniques.

It is the purpose of this investigation to study multi-modal propagation in nonuniform ducts with flow. Published work dealing with this problem has been limited to approximate methods for nonuniformities in cross section, lining and flow properties which are slowly varying. Tam[7] considered hardwalled ducts with slowly varying cross section by using a Born type of approximation and Fourier Transform methods. Nayfeh and his co-workers[8] have used the method of multiple scales and include slowly varying area, lining and boundary layer. While Tam's work allows modal coupling, Nayfeh's does not.

The method described here treats the complete acoustic field equations and is approximate only in the sense that the solutions are represented in terms of a superposition of a limited number of specified functions. We will be concerned primarily with the method of solving the field equations and relatively little with the difficulty presented by describing the nonuniform steady flow field. Instead, we will use an approximation for the flow field based on one dimensional compressible flow

with a kinematic modification to allow for flow tangency at the duct walls.

In addition, in this initial study of computational schemes we will concentrate primarily on the solution in elementary duct sections. Rather than an exhaustive treatment of the transmission characteristics of various duct configurations we limit our attention to the successful implementation of the scheme in particular cases.

A principal motivation for the study of propagation in ducts with flow is the observed phenomenon of subsonic acoustic choking which occurs in inlet type flows when the acoustic source radiates upstream through a flow constriction. It is found that there is a substantial reduction in acoustic transmission past the constriction when the Mach number in the constriction exceeds about $M = 0.7$. One would predict this intuitively if the constriction is sonic; however, the occurence of acoustic choking at such low Mach number is surprising and requires investigation. Tam[9] has considered the possibility that some of the choking is attributable to nonlinear effects arising when high intensity sound propagates upstream. The computational scheme developed in this paper provides a basis for studying the linear aspects of this problem. Extensive computations directed toward this goal will be made in an extension of the current research effort.

CO-ORDINATE SYSTEM AND GEOMETRY

In the following development we will consider only two dimensional ducts. The method employed generalizes to the three dimensional case, but is then, of course, more computationally demanding. We will also consider explicitly only ducts of infinite length, although as has been shown[1], the extension to ducts which are of finite length is not difficult provided that the reflection properties of the termination are known.

Figure 1 shows the type of configuration under consideration in which two semi-infinite uniform duct sections of height b_0 and b_ℓ are joined by a transition section of variable height $b(x)$. The duct wall at $y = 0$ is hard and the wall at $y = b(x)$ in the transition section has variable impedance $Z_0(x)$. The uniform sections have impedance Z_0 and Z_ℓ at $y = b_0$ and $y = b_\ell$, respectively, and have a hard wall at $y = 0$.

This representation can be considered as a model of a duct of this configuration or of one symmetric with respect to the x axis with symmetric propagation. We will consider only continuous variations in duct height; however discontinuous changes in impedance will be permitted at the ends of the nonuniformity.

GOVERNING ACOUSTIC EQUATIONS

We will consider acoustic propagation as small perturbations on the steady duct flow. It is assumed in the present analysis that the fluid motion is nonviscous and isentropic. To derive the acoustic equations we begin with the equations of continuity, momentum, energy and state in dimensional form

$$\frac{\partial \rho'}{\partial t} + div\, \rho' \vec{V}' = 0 \tag{1}$$

$$\rho' \frac{\partial \vec{V}'}{dt} + \rho' \vec{V}' \cdot grad\, \vec{V}' = - grad\, p \tag{2}$$

$$\frac{\partial p'}{\partial t} + \vec{V}' \cdot grad\, p' + \gamma p' div\, \vec{V}' = 0 \tag{3}$$

$$\frac{p'}{p_r} = \left(\frac{\rho'}{\rho_r}\right)^{\gamma} \tag{4}$$

The fluid state variables ρ', p', $\bar{v}'$ are made up of small acoustic perturbations on the steady flow, so that

$$\rho' = \rho_o^* + \rho^* \tag{5}$$

$$p' = p_o^* + p^* \tag{6}$$

$$\vec{V}' = \vec{V}_o^* + \vec{V}^* \tag{7}$$

where ρ^*_o, p^*_o, $\bar{v}^*_o$ are the steady flow conditions defined by

$$div\, \rho_o^* \vec{V}_o^* = 0 \tag{8}$$

$$\rho_o^* \vec{V}_o^* \cdot grad\, \vec{V}_o^* = - grad\, p_o^* \tag{9}$$

$$\vec{V}_o^* \cdot grad\, p_o^* + \gamma p_o^* div\, V_o^* = 0 \tag{10}$$

$$\frac{p_o^*}{p_r} = \left(\frac{\rho_o^*}{\rho_r}\right)^{\gamma} \tag{11}$$

Because of the isentropic assumption the energy equation is directly derivable from the continuity equation. The energy equation does not contain the density and is more convenient to use. By using Equations (5) - (7) in Equations (2) - (4) and by making the acoustic assumption of small perturbations on the steady flow, the dimensional acoustic momentum, energy and state equations are:

$$\rho_0^* \frac{\partial \vec{V}^*}{\partial t} + \rho_0^* \vec{V}^* \cdot \text{grad}\, \vec{V}_0^* + \rho^* \vec{V}_0^* \cdot \text{grad}\, \vec{V}_0^* + \rho_0^* \vec{V}_0^* \cdot \text{grad}\, \vec{V}^* = -\text{grad}\, p^* \tag{12}$$

$$\frac{\partial p^*}{\partial t} + \vec{V}_0^* \cdot \text{grad}\, p^* + \gamma p_0^* \,\text{div}\, \vec{V}^* + \vec{V}^* \cdot \text{grad}\, p_0^* + \gamma p^* \,\text{div}\, \vec{V}_0^* = 0 \tag{13}$$

$$p^* = \gamma \frac{p_0^*}{\rho_0^*} \rho^* = c^{*2} \rho^* \tag{14}$$

Equations (9) and (10) were used to eliminate the steady flow terms in Equations (12) and (13). The term in Equation (12) containing ρ^* can be rewritten by using Equation (14) and equation (9):

$$\rho^* \vec{V}_0^* \cdot \text{grad}\, \vec{V}_0^* = -\frac{1}{\gamma} \frac{p^*}{p_0^*} \text{grad}\, p_0^*$$

The modified momentum equation is then

$$\rho_0^* \frac{\partial \vec{V}^*}{\partial t} + \rho_0^* \vec{V}^* \cdot \text{grad}\, \vec{V}_0^* + \rho_0^* \vec{V}_0^* \cdot \text{grad}\, \vec{V}^* + \text{grad}\, p^* - \frac{1}{\gamma} \frac{p^*}{p_0^*} \text{grad}\, p_0^* = 0 \tag{15}$$

The governing acoustic equations can be non-dimensionalized in the standard way by defining the nondimensional variables.

$$p = \frac{p^*}{\rho_r c_r^2} \quad , \quad p_0 = \frac{p_0^*}{\rho_r c_r^2} \quad , \quad \rho = \frac{\rho^*}{\rho_r}$$

$$\rho_0 = \frac{\rho_0^*}{\rho_r} \quad , \quad \vec{V} = \frac{\vec{V}^*}{c_r} \quad , \quad \vec{V}_0 = \frac{\vec{V}_0^*}{c_r}$$

The reference states ρ_r, c_r are arbitrary values of the density and speed of sound. They will generally be chosen as the state which exists in the uniform flow incident on the nonuniformity. The nondimensional equations of momentum, energy and state are then

$$\frac{1}{c_r} \frac{\partial \vec{V}}{\partial t} + \vec{V} \cdot \text{grad}\, \vec{V}_0 + \vec{V}_0 \cdot \text{grad}\, \vec{V} + \frac{1}{\rho_0} \text{grad}\, p - \frac{1}{\gamma} \frac{p}{p_0 \rho_0} \text{grad}\, p_0 = 0 \tag{16}$$

$$\frac{1}{c_r} \frac{\partial p}{\partial t} + \vec{V}_0 \cdot \text{grad}\, p + \gamma p_0 \,\text{div}\, \vec{V} + \vec{V} \cdot \text{grad}\, p_0 + \gamma p \,\text{div}\, \vec{V}_0 = 0 \tag{17}$$

$$p = \gamma \frac{p_0}{\rho_0} \rho \tag{18}$$

When a harmonic time dependence of the form $e^{i\omega t}$ is assumed, Equations (16) and (17) become

$$ik_r \vec{V} + \vec{V} \cdot grad\, \vec{V}_0 + \vec{V}_0 \cdot grad\, \vec{V} + \frac{1}{\rho_0} grad\, p - \frac{1}{\gamma} \frac{\mathcal{P}}{p_0 \rho_0} grad\, p_0 = 0 \qquad (19)$$

$$ik_r p + \vec{V}_0 \cdot grad\, p + \gamma p_0\, div\, \vec{V} + \vec{V} \cdot grad\, p + \gamma p\, div\, \vec{V}_0 = 0 \qquad (20)$$

where $k_r = \omega / c_r = 2\pi/\lambda_r$ and λ_r is the free space wave number in the reference state.

In order to specify a boundary condition at the duct walls, we introduce a co-ordinate system as shown in Figure 1. This figure shows the manner in which the duct height profile and slope of the height profile are specified as well as the designation of the local outward unit normal at the duct wall, $\vec{\nu}$. The duct wall boundary condition employed is characteristic of a normally reacting lining in the presence of a harmonic pressure variation,

$$p^* = Z v_\nu^*$$

where v^*_υ is the particle velocity in the acoustic lining at the surface, assumed in the direction of the outward normal. Z is the wall impedance which may be a function of axial position. In nondimensional variables the boundary condition becomes

$$p = \frac{Z}{\rho_r c_r} v_\nu$$

or

$$v_\nu = A p$$

where $A = \rho_r c_r / Z$ is the acoustic admittance ratio of the lining based on the reference admittance $1/\rho_r c_r$. In harmonic motion the relation between the component of fluid particle velocity at the wall and particle velocity in the lining at the wall is given by

$$\vec{V}^* \cdot \vec{\nu} = v_\nu^* + u_\tau^* \frac{\partial}{\partial \tau} \left(\frac{v_\nu^*}{i\omega} \right)$$

u_τ^* is the fluid velocity tangent to the wall and $\frac{\partial}{\partial \tau}$ is the directional derivative along the wall. In nondimensional form this becomes

$$\vec{V} \cdot \vec{\nu} = v_\nu + \frac{u_\tau}{ik_r} \frac{\partial v_\nu}{\partial \tau} \qquad (21)$$

The boundary condition at a duct wall, assuming a time dependence $e^{i\omega t}$, is thus

$$\vec{V}\cdot\vec{\nu} = Ap - \frac{U_r}{k_r}\frac{\partial}{\partial\tau}(Ap)$$

Equations (19) and (20) with the duct wall boundary condition of Equation (21) specify the boundary value problem for propagation in a variable geometry duct with a steady flow. The problem as described is formidable, principally due to the introduction of the steady duct flow. The introduction of the flow field considerably complicates the acoustic problem, but it also presents the requirement of describing the flow field. The flow field would be defined by the solution of Equations (8) - (11) plus suitable boundary conditions. Even for simple duct geometries this requires sophisticated numerical techniques and only rarely in highly specialised cases could one hope to generate an exact closed form solution. For detailed studies a fairly exact description of the flow field may be required. However, in order to study the effect of duct nonuniformities on the propagation of sound with a certain degree of generality, we will use an approximation to the steady flow field.

The most common approximate description of the steady flow field is the one-dimensional theory which is one of the cornerstones of elementary gasdynamics. This theory proves very useful for a wide range of duct contours, but with rigor must be viewed as a first approximation when the area change is gradual.

In the one-dimensional theory the variation of the Mach number, nondimensional density and pressure with axial position are given by

$$\frac{dM_0}{dx} = -\frac{M_0}{1-M_0^2}\left[1+\frac{\gamma-1}{2}M_0^2\right]\frac{1}{A_c}\frac{dA_c}{dx}$$

$$\rho_0 = \frac{\rho_0^*}{\rho_r} = \frac{\left[1+\frac{\gamma-1}{2}M_r^2\right]^{\frac{1}{\gamma-1}}}{\left[1+\frac{\gamma-1}{2}M_0^2\right]^{\frac{1}{\gamma-1}}}$$

$$p_0 = \frac{p_0^*}{\rho_r c_r^2} = \frac{1}{\gamma}\frac{\left[1+\frac{\gamma-1}{2}M_r^2\right]^{\frac{\gamma}{\gamma-1}}}{\left[1+\frac{\gamma-1}{2}M_0^2\right]^{\frac{\gamma}{\gamma-1}}}$$

where A_c is the local cross sectional area.

In addition, the local nondimensional speed of sound is given by:

$$c_o^2 = \left(\frac{c_o^*}{c_r}\right)^2 = \frac{1 + \frac{\gamma-1}{2} M_r^2}{1 + \frac{\gamma-1}{2} M_o^2}$$

and the local nondimensional flow velocity is given by:

$$U_o = \frac{U_o^*}{c_r} = M_o \frac{\left[1 + \frac{\gamma-1}{2} M_o^2\right]^{1/2}}{\left[1 + \frac{\gamma-1}{2} M_r^2\right]^{1/2}}$$

U_o is the local axial component of flow, the transverse components being assumed zero in the one dimensional approximation.

In this approximation the flow properties are assumed to be uniform at a cross section with no transverse velocity. They are solutions of the one dimensional continuity and momentum equations

$$\frac{1}{\rho_o}\frac{d\rho_o}{dx} + \frac{1}{U_o}\frac{dU_o}{dx} + \frac{1}{A_c}\frac{dA_c}{dx} = 0$$

$$\frac{dp_o}{dx} = -\rho_o U_o \frac{dU_o}{dx}$$

together with the isentropic equation of state

$$\frac{p_o}{p_r} = \left(\frac{\rho_o}{\rho_r}\right)^{\gamma}$$

The acoustic problem, Equations (19) and (20), involves axial and transverse velocities and pressures as well as axial and transverse gradients. Furthermore, the boundary condition requires the velocity tangent to the wall. This required velocity field could be approximated simply by using the one dimensional theory and ignoring the transverse velocity and the transverse gradients. We choose to include some measure of the effect of transverse velocity and its gradient by taking the solution to Equations (8) - (11) to be, in nondimensional form for the two dimensional duct

$$U_o(x, y) = \bar{U}_o(x)$$

$$V_o(x, y) = \bar{U}_o(x)\frac{y}{b}\frac{db}{dx}$$

$$p_o(x, y) = \bar{p}_o(x)$$

$$c_o(x, y) = \bar{c}_o(x)$$

where a bar notation has been used to denote the one dimensional solution. This form for the steady flow field must be recognised as approximate, but it is considered to be a reasonable approximation in that it exactly satisfies both the continuity equation, Equation (8) and the x component of the exact momentum equation, Equation (9). The y component of Equation (9) is not satisfied exactly, but is satisfied on an average basis on the cross section of a duct symmetric with respect to the x axis. In addition, this solution satisfies the requirement of flow tangency at the duct wall.

By using this approximation we are introducing an error into Equations (19) and (20) since in those equations it is assumed that the flow field satisfies Equations (8) - (11). Based on the success of one dimensional nozzle theory, the axial velocity, pressure and density variations should be acceptable over a fairly wide range of duct shapes. The assumption for the transverse velocity is on a less firm basis, and will be more accurate for gradual area changes. In the absence of detailed information about the flow field it is felt that tha approximate flow field will be useful for identifying the important general properties of transmission in non-uniform ducts.

The steady pressure, density and axial velocity in the steady flow approximation are functions of x alone so that the steady flow field is described by $U_o(x)$, $V_o(x,y)$, $p_o(x)$, $\rho_o(x)$. In addition the transverse gradient $\partial V_o/\partial y$ is a function of x alone. These simplifications provide significant reductions in numerical computations. However, if more exact flow field descriptions are used these restrictions must be relaxed.

With this approximation for the flow field, the momentum and energy equations, Equations (19) and (20) can be expanded in the present two dimensional case to yield:

$$U_o \frac{\partial u}{\partial x} + \frac{1}{\rho_o}\frac{\partial p}{\partial x} + V_o \frac{\partial u}{\partial y} + \left(ik_r + \frac{\partial U_o}{\partial x}\right)u - \frac{1}{\gamma p_o \rho_o}\frac{\partial p_o}{\partial x}p = 0 \qquad (22)$$

$$U_o \frac{\partial v}{\partial x} + V_o \frac{\partial v}{\partial y} + \frac{1}{\rho_o}\frac{\partial p}{\partial y} + \frac{\partial V_o}{\partial x}u + \left(ik_r + \frac{\partial V_o}{\partial y}\right)v = 0 \qquad (23)$$

$$\gamma p_o \frac{\partial u}{\partial x} + U_o \frac{\partial p}{\partial x} + \gamma p_o \frac{\partial v}{\partial y} + V_o \frac{\partial p}{\partial y} + \frac{\partial p_o}{\partial x}u + \left[ik_r + \gamma\left(\frac{\partial U_o}{\partial x} + \frac{\partial V_o}{\partial y}\right)\right]p = 0 \qquad (24)$$

The boundary condition of Equation (21) can be expanded by noting that at the duct wall:

$$U_\tau = U_o \cos\theta + V_o \sin\theta$$

$$\frac{\partial}{\partial \tau}(Ap) = \cos\theta \frac{\partial}{\partial x}(Ap) + \sin\theta A \frac{\partial p}{\partial y}$$

Thus

$$U_\tau \frac{\partial}{\partial \tau}(Ap) = (U_o \cos^2\theta + V_o \sin\theta\cos\theta)\frac{\partial}{\partial x}(Ap)$$

$$+ (U_o \cos\theta \sin\theta + V_o \sin^2\theta) A \frac{\partial p}{\partial y}$$

The boundary condition at the wall for the steady flow is that the normal velocity must vanish:

$$0 = V_o \cos\theta - U_o \sin\theta$$

or

$$V_o = U_o \tan\theta$$

Thus, at the duct wall

$$U_\tau \frac{\partial}{\partial \tau}(Ap) = \left\{ U_o \frac{\partial}{\partial x}(Ap) + U_o \tan\theta A \frac{\partial p}{\partial y} \right\}$$

Furthermore

$$\vec{V} \cdot \vec{\nu} = v\cos\theta - u\sin\theta$$

Equation (21) becomes, at a duct wall

$$v\cos\theta - u\sin\theta = Ap - \frac{iU_o}{k_r}\left[\frac{\partial}{\partial x}(Ap) + \tan\theta A \frac{\partial p}{\partial y}\right] \tag{25}$$

METHOD OF SOLUTION IN THE NONUNIFORM SECTION

In Reference (1), the method of weighted residuals (MWR) (modified Galerkin method), was employed to study acoustic propagation in nonuniform ducts without flow. We will use this method with minor changes in the present study. (Reference (1) is reproduced in Appendix (A)).

Attention will be restricted to two dimensional ducts with geometry as shown in Fig. 1. As previously noted, this can be considered as a model for a duct actually shaped as shown or else one symmetric with respect to the x axis. In the latter case we consider only symmetric propagation.

We seek solutions to the field equations, Equations (22) - (24), and the boundary condition, Equation (25) in the form:

$$p(x,y) = \sum_n p_n(x)\,\psi_n(x,y)$$

$$u(x,y) = \sum_n u_n(x)\,\theta_n(x,y)$$

$$v(x,y) = \sum_n v_n(x)\,\phi_n(x,y)$$

The success of the MWR is dependent on an appropriate choice of basis functions. In the no flow case of Reference (1), the basis functions were chosen to be the transverse modal functions which would exist in a uniform duct with the properties existing locally in the nonuniform duct. This philosophy can be carried over to the duct with a steady mean flow. In this case the appropriate choice of basis functions would be the transverse modal functions for a uniform duct with flow and geometry properties existing locally in the nonuniform duct. In the nonuniform duct the flow properties vary transversely so that the equivalent uniform flow to be used in defining the basis functions is open to interpretation. Since the boundary residual will be more nearly satisified if the basis functions nearly satisy the boundary condition, it would seem appropriate to use the velocity at the wall as the equivalent uniform velocity. Of course in the simple flow model used here this is unimportant, since the wall velocity is the same as the velocity on the duct axis.

The major disadvantage to using this type of basis function is that there are different modes for upstream and downstream propagation so that to obtain the same resolution as in the no flow case we would use twice as many modes, half representing upstream propagation and half representing downstream propagation.

A second possibility would be the use of the no flow modes. Since these modes are not generally near-solutions we would expect to generate solutions which require a large number of terms to converge. We tried using the no flow modes in the initial development and found that they worked well at low Mach numbers with soft walls and for nearly hard walls. In both instances the no flow and flow transverse modal functions are not

much different so that this success is not unexpected. For this reason we have one version of the computational scheme for nearly hard walls or for soft walls at low Mach number. We will detail here the more general case.

Using the basis functions from uniform duct theory (with flow), solutions are sought in the form:

$$p_N = \sum_{n=1}^{N} p_n(x)\cos\kappa_n y = \sum_{n=1}^{N} p_n \psi_n$$

$$u_N = \sum_{n=1}^{N} u_n(x)\cos\kappa_n y = \sum_{n=1}^{N} u_n \psi_n$$

$$v_N = \sum_{n=1}^{N} v_n(x)\sin\kappa_n y = \sum_{n=1}^{N} v_n \phi_n$$

The κ_n are defined by:

$$\kappa b \tan \kappa b = ikbA\left(1 - M\frac{k_x}{k}\right)^2$$

$$\frac{k_x}{k} = \frac{1}{1-M^2}\left[-M \pm \sqrt{1-(1-M^2)\left(\frac{\kappa}{k}\right)^2}\right]$$

The Mach number to use is that which exists at the duct wall. This eigenvalue problem simultaneously yields the transverse wave number and k_{x_n} for a mode of propagation. Eigenvalues for propagation in both the plus and minus axial direction will appear and will be identified by the sign in k_{x_n}.

The eigenfunctions which arise in the flow case are not orthogonal and the orthogonality property cannot be used in computations. However, in the flow case this disadvantage is not of serious consequence in view of the other complexity which already exists.

If the assumed solution is substituted in the differential equations, Equations (22) - (24), it will in general not satisfy them and the left hand side will not equate to zero. Instead, it will add up to an error, or residual. By denoting the residual by R, we write upon substituting the assumed solution in the governing equations:

$$R_1 = U_o \frac{\partial u_N}{\partial x} + \frac{1}{\rho_o}\frac{\partial p_N}{\partial x} + V_o \frac{\partial u_N}{\partial y} + \left(ik_r + \frac{\partial U_o}{\partial x}\right) u_N - \frac{1}{\gamma p_o \rho_o}\frac{\partial p_o}{\partial x} p_N$$

$$R_2 = U_o \frac{\partial v_N}{\partial x} + V_o \frac{\partial v_N}{\partial y} + \frac{1}{\rho_o}\frac{\partial p_N}{\partial y} + \frac{\partial V_o}{\partial x} u_N + \left(ik_r + \frac{\partial V_o}{\partial y}\right) v_N$$

$$R_3 = \gamma p_o \frac{\partial u_N}{\partial x} + U_o \frac{\partial p_N}{\partial x} + \gamma p_o \frac{\partial v_N}{\partial y} + V_o \frac{\partial p_N}{\partial y} + \frac{\partial p_o}{\partial x} u_N + \left[ik_r + \gamma\left(\frac{\partial U_o}{\partial x} + \frac{\partial V_o}{\partial y}\right)\right] p_N$$

In a similar manner we form a boundary residual.

$$R_B = v_N \cos\theta - u_N \sin\theta - A\left\{p_N - \frac{iU_o}{k_r}\left[\frac{\partial p_N}{\partial x} + \tan\theta \frac{\partial p_N}{\partial y} + \frac{p_N}{A}\frac{dA}{dx}\right]\right\}$$

The residuals can be made zero if they are orthogonal to every member of a complete set. (See Eversman, Cook and Beckemeyer [1], Finlaysan [10] and Zinn and Powell [11,12]). Assuming that the trial functions $\psi_n(x,y)$, $\phi_n(x,y)$ are complete sets at every value of x we can force

$$\int_0^1 \int_0^b \psi_n R_1 \, dy \, dz = 0$$

$$\int_0^1 \int_0^b \phi_n R_2 \, dy \, dz = 0$$

$$\int_0^1 \int_0^b \psi_n R_3 \, dy \, dz = 0$$

$$\int_0^1 \psi_n R_B \, dz = 0$$

$n = 1, 2, 3, \cdots N$

A unit depth of the duct is assumed. Note that the trial functions already satisfy the boundary condition at the hard wall (or duct centre line) so that no boundary residual is required there. In expanded form the orthogoniality conditions for the differential equations yield

$$U_0\int_0^b \psi_n \frac{\partial u_N}{\partial x}\,dy + \frac{1}{\rho_0}\int_0^b \psi_n \frac{\partial p_N}{\partial x}\,dy + \int_0^b V_0\,\psi_n \frac{\partial u_N}{\partial y}\,dy + (ik_r + \frac{\partial U_0}{\partial x})\int_0^b \psi_n u_N\,dy - \frac{1}{\gamma p_0 \rho_0}\frac{\partial p_0}{\partial x}\int_0^b \psi_n p_N\,dy = 0 \qquad (26)$$

$$U_0\int_0^b \phi_n \frac{\partial v_N}{\partial x}\,dy + \int_0^b V_0\,\phi_n \frac{\partial v_N}{\partial y}\,dy + \frac{1}{\rho_0}\int_0^b \phi_n \frac{\partial p_N}{\partial y}\,dy + \int_0^b \frac{\partial V_0}{\partial x}\,\phi_n u_N\,dy + (ik_r + \frac{\partial V_0}{\partial y})\int_0^b \phi_n v_N\,dy = 0 \qquad (27)$$

$$\gamma p_0\int_0^b \psi_n \frac{\partial u_N}{\partial x}\,dy + U_0\int_0^b \psi_n \frac{\partial p_N}{\partial x}\,dy + \gamma p_0\int_0^b \psi_n \frac{\partial v_N}{\partial y}\,dy + \int_0^b V_0\,\psi_n \frac{\partial p_N}{\partial y}\,dy + \frac{\partial p_0}{\partial x}\int_0^b \psi_n u_N\,dy + [ik_r + \gamma(\frac{\partial U_0}{\partial x} + \frac{\partial V_0}{\partial y})]\int_0^b \psi_n p_N\,dy = 0 \qquad (28)$$

$$n = 1, 2, \cdots N$$

Equations (26), (27), (28) can be rewritten and simplified to some extent by following the sequence of steps outlined in Reference (1) (See Appendix A of the present document). We use rules for differentiation of integrals, integration by parts, and the condition of flow tangency at the wall to obtain new forms of Equations (26) and (27) for n = 1,2,...N:

$$U_o \frac{d}{dx}\int_o^b \psi_n u_N\, dy + \frac{1}{\rho_o}\frac{d}{dx}\int_o^b \psi_n p_N\, dy - U_o\int_o^b \frac{\partial \psi_n}{\partial x} u_N\, dy - \frac{1}{\rho_o}\int_o^b \frac{\partial \psi_n}{\partial x} p_N\, dy$$

$$-\int_o^b \frac{\partial}{\partial y}(V_o \psi_n) u_N\, dy + (ik_r + \frac{\partial U_o}{\partial x})\int_o^b \psi_n u_N\, dy - \frac{1}{\gamma p_o \rho_o}\frac{\partial p_o}{\partial x}\int_o^b \psi_n p_N\, dy$$

$$-\frac{1}{\rho_o}\psi_n(x,b) + \tan\theta\, p_N(x,b) = 0 \qquad (29)$$

$$U_o \frac{d}{dx}\int_o^b \phi_n v_N\, dy - U_o\int_o^b \frac{\partial \phi_n}{\partial x} v_N - \int_o^b \frac{\partial}{\partial y}(V_o \phi_n) v_N\, dy - \frac{1}{\rho_o}\int_o^b \frac{\partial \phi_n}{\partial y} p_N\, dy$$

$$+\int_o^b \frac{\partial V_o}{\partial x}\phi_n u_N\, dy + (ik_r + \frac{\partial V_o}{\partial y})\int_o^b \phi_n v_N\, dy$$

$$+\frac{1}{\rho_o}\phi_n(x,b) p_N(x,b) = 0 \qquad (30)$$

The weighted boundary residual takes the form

$$[v_N(x,b) - u_N(x,b)\tan\theta]\psi_n(x,b)$$

$$= \frac{A}{\cos\theta}\left\{p_N - \frac{iU_o}{k_r}\left[\frac{\partial p_N}{\partial x} + \tan\theta\frac{\partial p_N}{\partial y} + \frac{1}{A}\frac{dA}{dx}p_N\right]\right\}_{y=b}\psi_n(x,b)$$

By using the steps outlined above, plus the boundary residual. Equation (28) is rewritten for n = 1,2,...N

$$\gamma p_o \frac{d}{dx}\int_o^b \psi_n u_N dy + U_o \frac{d}{dx}\int_o^b \psi_n p_N dy - \gamma p_o \int_o^b \frac{\partial \psi_n}{\partial x} u_N dy - U_o \int_o^b \frac{\partial \psi_n}{\partial x} p_N dy$$

$$-\gamma p_o \int_o^b \frac{\partial \psi_n}{\partial y} v_N dy - \int_o^b \frac{\partial}{\partial y}(V_o \psi_n) p_N dy + \frac{\partial p_o}{\partial x}\int_o^b \psi_n u_N dy$$

$$+\left[ik_r + \sigma\left(\frac{\partial u_o}{\partial x} + \frac{\partial v_o}{\partial y}\right)\right]\int_o^b \psi_n p_N \, dy$$

$$+ \gamma p_o \frac{A}{\cos\theta}\left\{p_N - \frac{iu_o}{k_r}\left[\frac{\partial p_N}{\partial x} + \tan\theta \frac{\partial p_N}{\partial y} + \frac{1}{A}\frac{dA}{dx} p_N\right]\right\}_{y=b} \psi_n(x,b) = 0 \qquad (31)$$

The Method of Weighted Residuals can be completed by inserting in Equations (29), (30), and (31) the truncated series representations for p_N, u_N, v_N. If this is done and the terms are grouped there results

$$u_o \sum_m N_{nm} \frac{du_m}{dx} + \frac{1}{\rho_o} \sum_m N_{nm} \frac{dp_m}{dx}$$

$$+ \sum_m \left[u_o \frac{dN_{nm}}{dx} + \left(ik_r + \frac{\partial u_o}{\partial x}\right) N_{nm} - \int_o^b \frac{\partial}{\partial y}(v_o \psi_n)\psi_m dy - u_o \int_o^b \frac{\partial \psi_n}{\partial x} \psi_m dy \right] u_m$$

$$+ \sum_m \left[\frac{1}{\rho_o} \frac{dN_{nm}}{dx} - \frac{1}{\rho_o} \int_o^b \frac{\partial \psi_n}{\partial x} \psi_m \, dy - \frac{1}{\gamma p_o \rho_o} \frac{\partial p_o}{\partial x} N_{nm} - \frac{1}{\rho_o} \tan\theta \, \psi_n(x,b)\psi_m(x,b) \right] p_m = 0$$

(32)

$$u_o \sum_m M_{nm} \frac{dv_m}{dx}$$

$$+ \sum_m \left[u_o \frac{dM_{nm}}{dx} + \left(ik_r + \frac{\partial v_o}{\partial y}\right) M_{nm} - u_o \int_o^b \frac{\partial \phi_n}{\partial x} \phi_m \, dy - \int_o^b \frac{\partial}{\partial y}(v_o \phi_n)\phi_m \, dy \right] v_m$$

$$+ \sum_m \int_o^b \frac{\partial v_o}{\partial x} \phi_n \psi_m \, dy \, u_m$$

$$+ \sum_m \left[\frac{1}{\rho_o} \phi_n(x,b)\psi_m(x,b) - \frac{1}{\rho_o} \int_o^b \frac{\partial \phi_n}{\partial y} \psi_m \, dy \right] p_m = 0$$

(33)

$$\gamma p_o \sum_m N_{nm} \frac{du_m}{dx} + \sum_m \left[u_o N_{nm} - \frac{i u_o}{k_r} \frac{\gamma p_o}{\cos\theta} A \psi_n(x,b) \psi_m(x,b) \right] \frac{dp_m}{dx}$$

$$- \sum_m \gamma p_o \int_o^b \frac{\partial \psi_n}{\partial y} \phi_m \, dy \; v_m$$

$$+ \sum_m \left[\gamma p_o \frac{dN_{nm}}{dx} + \frac{dp_o}{dx} N_{nm} - \gamma p_o \int_o^b \frac{\partial \psi_n}{\partial x} \psi_m \, dy \right] u_m$$

$$+ \sum_m \left\{ u_o \frac{dN_{nm}}{dx} + \left[i k_r + \gamma \left(\frac{\partial u_o}{\partial x} + \frac{\partial v_o}{\partial y} \right) \right] N_{nm} - \int_o^b \frac{\partial}{\partial y} (v_o \psi_n) \psi_m \, dy \right.$$

$$- u_o \int_o^b \frac{\partial \psi_n}{\partial x} \psi_m \, dy + \frac{\gamma p_o}{\cos\theta} A \left[\psi_n(x,b) \psi_m(x,b) - \frac{i u_o}{k_r} \left\{ \psi_n(x,b) \frac{\partial \psi_m(x,b)}{\partial x} \right. \right.$$

$$\left. \left. \left. + \tan\theta \, \psi_n(x,b) \frac{\partial \psi_m(x,b)}{\partial y} + \frac{1}{A} \frac{dA}{dx} \psi_n(x,b) \psi_m(x,b) \right\} \right] \right\} p_m = 0$$

(34)

Equation (34) required special consideration in that the terms contributed by the boundary residual yield derivatives of p_m (this did not occur in the no-flow case). We have introduced the definitions

$$N_{nm}(x) = \int_o^b \psi_n \psi_m \, dy$$

$$M_{nm}(x) = \int_o^b \phi_n \phi_m \, dy$$

Equations (32) - (34) can be written in the form

$$\gamma p_o \sum_m N_{nm} \frac{du_m}{dx} + u_o \sum_m \bar{N}_{nm} \frac{dp_m}{dx} + \sum_m U^u_{nm} u_m + \sum_m U^p_{nm} p_m + \sum_m U^v_{nm} v_m = 0$$

$$u_o \sum_m N_{nm} \frac{du_m}{dx} + \frac{1}{\rho_o} \sum_m N_{nm} \frac{dp_m}{dx} + \sum_m P^u_{nm} u_m + \sum_m P^p_{nm} p_m + \sum_m P^v_{nm} v_m = 0$$

$$u_o \sum_m M_{nm} \frac{dv_m}{dx} + \sum_m V^u_{nm} u_m + \sum_m V^p_{nm} p_m + \sum_m V^v_{nm} v_m = 0$$

(35)

We make use of the definitions of the basis functions

$$\psi_n(x,y) = \cos \kappa_n y$$

$$\phi_n(x,y) = \sin \kappa_n y \quad ,$$

the d rivative relations

$$\frac{\partial \phi_n}{\partial x} = \frac{d\kappa_n}{dx} y \, \psi_n(x,y)$$

$$\frac{\partial \phi_n}{\partial y} = \kappa_n \psi_n(x,y)$$

$$\frac{\partial \psi_n}{\partial x} = -\frac{d\kappa_n}{dx} y \, \phi_n(x,y)$$

$$\frac{\partial \psi_n}{\partial y} = -\kappa_n \phi_n(x,y)$$

and the definitions

$$\int_0^b y \, \phi_n \psi_m \, dy = L_{nm}$$

$$\int_0^b y \, \psi_n \phi_m \, dy = J_{nm} = L_{mn}$$

In addition, we use the description of the flow field to obtain

$$\int_0^b V_0 \phi_n \psi_m \, dy = U_0 \frac{1}{b} \frac{db}{dx} L_{nm}$$

$$\int_0^b V_0 \psi_n \phi_m \, dy = U_0 \frac{1}{b} \frac{db}{dx} J_{nm}$$

$$\int_0^b \frac{\partial V_0}{\partial y}\,\psi_n\,\psi_m\,dy = U_0\,\frac{1}{b}\,\frac{db}{dx}\,N_{nm}$$

$$\int_0^b \frac{\partial V_0}{\partial y}\,\phi_n\,\phi_m\,dy = U_0\,\frac{1}{b}\,\frac{db}{dx}\,M_{nm}$$

$$\int_0^b \frac{\partial V_0}{\partial x}\,\phi_n\,\psi_m\,dy = U_0\left[\frac{1}{U_0}\frac{dU_0}{dx}\frac{1}{b}\frac{db}{dx} + \frac{1}{b}\frac{d^2b}{dx^2} - \left(\frac{1}{b}\frac{db}{dx}\right)^2\right]L_{nm}$$

Using these relations, we arrive at definitions of the coefficients in Eqs (35):

$$\bar{N}_{nm} = N_{nm} - \frac{i}{k_r}\,\frac{\gamma p_0}{\cos\theta}\,A\,\psi_n(x,b)\,\psi_m(x,b)$$

$$U^u_{nm} = \gamma p_0\left[\frac{dN_{nm}}{dx} + \frac{d\kappa_n}{dx}\,L_{nm}\right] + \frac{dp_0}{dx}\,N_{nm}$$

$$U^p_{nm} = U_0\left[\frac{dN_{nm}}{dx} - \frac{1}{b}\frac{db}{dx}\,N_{nm}\right] + \left[ik_r + \gamma\left(\frac{dU_0}{dx} + \frac{\partial V_0}{\partial y}\right)\right]N_{nm}$$

$$+ U_0\,\frac{1}{b}\,\frac{d\kappa_n b}{dx}\,L_{nm} + \frac{\gamma p_0}{\cos\theta}\,A\left\{1 + \frac{iU_0}{k_r}\left[\frac{d\kappa_m b}{dx}\tan\kappa_m b - \frac{1}{A}\,\frac{dA}{dx}\right]\right\}\cos\kappa_n b\cos\kappa_m b$$

$$U^v_{nm} = \gamma p_0\,\kappa_n\,M_{nm}$$

$$P_{nm}^{u} = U_o\left[\frac{dN_{nm}}{dx} - \frac{1}{b}\frac{db}{dx}N_{nm}\right] + \left(ik_r + \frac{dU_o}{dx}\right)N_{nm}$$

$$+ U_o\frac{1}{b}\frac{d\kappa_n b}{dx}L_{nm}$$

$$P_{nm}^{p} = \frac{1}{\rho_o}\left[\frac{dN_{nm}}{dx} + \frac{d}{dx}\kappa_n L_{nm}\right] - \frac{1}{\gamma p_o \rho_o}\frac{dp_o}{dx}N_{nm}$$

$$- \frac{1}{\rho_o}\frac{db}{dx}\cos\kappa_n b\cos\kappa_m b$$

$$P_{nm}^{v} = 0$$

$$V_{nm}^{u} = U_o\left[\frac{1}{U_o}\frac{dU_o}{dx}\frac{1}{b}\frac{db}{dx} + \frac{1}{b}\frac{d^2b}{dx^2} - \left(\frac{1}{b}\frac{db}{dx}\right)^2\right]L_{nm}$$

$$V_{nm}^{p} = \frac{1}{\rho_o}\left[\sin\kappa_n b\cos\kappa_m b - \kappa_n N_{nm}\right]$$

$$V_{nm}^{v} = U_o\left[\frac{dM_{nm}}{dx} - \frac{1}{b}\frac{db}{dx}M_{nm}\right] + \left(ik_r + \frac{\partial V_o}{\partial y}\right)M_{nm}$$

$$- U_o\frac{1}{b}\frac{d\kappa_n b}{dx}J_{nm}$$

Equations (35) can be conveniently written in matrix form

$$\begin{bmatrix} \gamma p_o N_{nm} & U_o \bar{N}_{nm} & 0 \\ U_o N_{nm} & \frac{1}{\rho_o}N_{nm} & 0 \\ 0 & 0 & U_o M_{nm} \end{bmatrix} \begin{Bmatrix} \frac{du_m}{dx} \\ \frac{dp_m}{dx} \\ \frac{dv_m}{dx} \end{Bmatrix}$$

$$= \begin{bmatrix} -U_{nm}^{u} & -U_{nm}^{p} & -U_{nm}^{v} \\ -P_{nm}^{u} & -P_{nm}^{p} & -P_{nm}^{v} \\ -V_{nm}^{u} & -V_{nm}^{p} & -V_{nm}^{v} \end{bmatrix} \begin{Bmatrix} u_m \\ p_m \\ v_m \end{Bmatrix}$$

In order to achieve a form more closely related to the no flow equations, we divide the U_m equations by γp_0, multiply the p_m equations by ρ_0 and divide the v_m equations by U_0.

Hence we can write

$$\begin{bmatrix} N_{nm} & \frac{U_0}{\gamma p_0}\bar{N}_{nm} & 0 \\ U_0 N_{nm} & N_{nm} & 0 \\ 0 & 0 & M_{nm} \end{bmatrix} \begin{Bmatrix} \frac{du_m}{dx} \\ \frac{dp_m}{dx} \\ \frac{dv_m}{dx} \end{Bmatrix}$$

$$= \begin{bmatrix} -\bar{U}_{nm}^{u} & -\bar{U}_{nm}^{p} & -\bar{U}_{nm}^{v} \\ -\bar{P}_{nm}^{u} & -\bar{P}_{nm}^{p} & -\bar{P}_{nm}^{v} \\ -\bar{V}_{nm}^{u} & -\bar{V}_{nm}^{p} & -\bar{V}_{nm}^{v} \end{bmatrix} \begin{Bmatrix} u_m \\ p_m \\ v_m \end{Bmatrix} \qquad (36)$$

where

$$\bar{U}_{nm}^{u,p,v} = \frac{1}{\gamma p_0} U_{nm}^{u,p,v}$$

$$\bar{P}_{nm}^{u,p,v} = \rho_0 P_{nm}^{u,p,v}$$

$$\bar{V}_{nm}^{u,p,v} = \frac{1}{U_0} V_{nm}^{u,p,v}$$

Thus

$$\bar{U}_{nm}^{u} = \frac{dN_{nm}}{dx} + \frac{d\kappa_n}{dx} L_{nm} + \frac{1}{\gamma p_0}\frac{dp_0}{dx} N_{nm}$$

$$\bar{U}_{nm}^{p} = \frac{U_0}{\gamma p_0}\left[\frac{dN_{nm}}{dx} - \frac{1}{b}\frac{db}{dx} N_{nm}\right] + \frac{1}{\gamma p_0}\left[ik_r + \gamma\left(\frac{dU_0}{dx} + \frac{\partial V_0}{\partial y}\right)\right] N_{nm}$$

$$+ \frac{U_0}{\gamma p_0}\frac{1}{b}\frac{d\kappa_n b}{dx} L_{nm} + \frac{A}{\cos\theta}\left\{1 + \frac{iU_0}{k_r}\left[\frac{d\kappa_m b}{dx} + \alpha\kappa_m b\right.\right.$$

$$\left.\left. - \frac{1}{A}\frac{dA}{dx}\right]\right\} \cos\kappa_n b \cos\kappa_m b$$

$$\bar{U}^{v}_{nm} = \kappa_n M_{nm}$$

$$\bar{P}^{u}_{nm} = \rho_o U_o \left[\frac{dN_{nm}}{dx} - \frac{1}{b}\frac{db}{dx} N_{nm} \right] + \rho_o \left(ik_r + \frac{dU_o}{dx} \right) N_{nm}$$

$$+ \rho_o U_o \frac{1}{b} \frac{d\kappa_n b}{dx} L_{nm}$$

$$\bar{P}^{p}_{nm} = \frac{dN_{nm}}{dx} + \frac{d\kappa_n}{dx} L_{nm} - \frac{1}{\gamma p_o} \frac{dp}{dx} N_{nm}$$

$$- \frac{db}{dx} \cos \kappa_n b \cos \kappa_m b$$

$$\bar{P}^{v}_{nm} = 0$$

$$\bar{V}^{u}_{nm} = \left[\frac{1}{U_o} \frac{dU_o}{dx} \frac{1}{b} \frac{db}{dx} + \frac{1}{b} \frac{d^2 b}{dx^2} - \left(\frac{1}{b} \frac{db}{dx} \right)^2 \right] L_{nm}$$

$$\bar{V}^{p}_{nm} = \frac{1}{\rho_o U_o} \left[\sin \kappa_n b \cos \kappa_m b - \kappa_n N_{nm} \right]$$

$$\bar{V}^{v}_{nm} = \frac{dM_{nm}}{dx} - \frac{1}{b}\frac{db}{dx} M_{nm} + \frac{1}{U_o} \left(ik_r + \frac{\partial V_o}{\partial y} \right) M_{nm}$$

$$- \frac{1}{b} \frac{d\kappa_n b}{dx} J_{nm}$$

MATCHING OF THE NONUNIFORM SECTION TO UNIFORM SECTIONS

As illustrated in Figure 1, the nonuniform duct segment is considered to be a transition section between two uniform, infinite ducts. In this section we establish the procedure for matching the nonuniformity to the uniform sections.

The set of linear ordinary differential equations for the axial variation of the coefficients in the assumed solution, given by Equation (36), can be represented in the form

$$\left[L(x)\right]\begin{Bmatrix} \frac{du_m}{dx} \\ \frac{dp_m}{dx} \\ \frac{dv_m}{dx} \end{Bmatrix} = \left[F(x)\right]\begin{Bmatrix} u_m \\ p_m \\ v_m \end{Bmatrix}$$

The dimensioning of the matrices involved depends on the types of basis functions used. In our investigations to date we have used three different types of basis functions:

(1) Initial studies utilized as basis functions the modes from the no-flow problem. In this case the assumed solution and the required eigenvalues are exactly as described in Reference (1) which is included in Appendix A to this document. The differential equation is then dimensioned as follows:

$$\underset{3N\times 3N}{\left[L(x)\right]}\underset{3N\times 1}{\begin{Bmatrix} \frac{du_m}{dx} \\ \frac{dp_m}{dx} \\ \frac{dv_m}{dx} \end{Bmatrix}} = \underset{3N\times 3N}{\left[F(x)\right]}\underset{3N\times 1}{\begin{Bmatrix} u_m \\ p_m \\ v_m \end{Bmatrix}}$$

N is the number of basis functions used. Note that in this form the problem is of size 3N x 3N as compared to 2N x 2N in the no-flow case. Extensive computations were carried out using this method and it was found to give results in generally good agreement with known correct results for low Mach numbers with soft walls and for a more extensive Mach number range with nearly hard walls. Computations using this approach form a large portion of the results generated to date and are discussed in a subsequent

section. As will be seen, certain inadequacies exist and we have extended the computational scheme to use modes more closely related to the flow problem. The details of this approach will not be given here as they can be inferred from the more sophisticated approaches to follow.

(2) Since the success of Galerkin type methods depends to a large extent on an appropriate choice of basis functions we have modified the basic computational scheme described above to use modes from uniform duct theory with the effects of flow included. In the first step in this direction we employed the flow modes but included only modes corresponding to propagation in the positive axial direction (in the flow case, as distinct from the no-flow case, there is one set of positive moving modes and another set of negative moving modes). This is really a sub-case of the more general use of the flow modes described below and as such will not be described separately. The dimensioning in this case is the same as the case when no-flow modes are used, however, the eigenvalues associated with the basis functions require a more extensive eigenvalue routine, as described in Appendix B.

(3) The most advanced version of the Galerkin method developed to date uses the full set of uniform duct flow modes, including both positive and negative running waves. The principal reason for avoiding this approach at the outset was the nominal doubling of the number of modes required. If we let N denote the number of positive running modes, then, since for each positive running mode there is a corresponding negative running one, we actually require 2N modes to achieve the same level of resolution used in the previously discussed cases. In this instance the dimensioning is

$$\underset{6N\times 6N}{[L(x)]}\underset{6N\times 1}{\begin{Bmatrix} \frac{du_m}{dx} \\ \frac{dp_m}{dx} \\ \frac{dv_m}{dx} \end{Bmatrix}} = \underset{6N\times 6N}{[F(x)]}\underset{6N\times 1}{\begin{Bmatrix} u_m \\ p_m \\ v_m \end{Bmatrix}} \qquad (37)$$

As noted, N is the number of modes in one direction and is a measure of the basis function resolution available, consistent with the other implementations. At the time of preparation of this document numerical experimentation to verify and improve this formulation is still in progress. Certain new computation problems have been observed and are currently under investigation. Hence, the use of the complete flow modes can at this stage only be considered in the development stage. However, since this formulation is the most general, we will use it to explain the matching procedure. The corresponding procedure in the simpler formulations can then be easily inferred.

The solution to the matrix differential equations of Eq. (36) can be given in terms of a transfer matrix relating u_n, p_n, v_n at $x = \ell$ to u_n, p_n, v_n at $x = 0$:

$$\underset{6N\times 1}{\begin{Bmatrix} u_n \\ p_n \\ v_n \end{Bmatrix}_{x=\ell}} = \underset{6N\times 6N}{[T]} \underset{6N\times 1}{\begin{Bmatrix} u_m \\ p_m \\ v_m \end{Bmatrix}_{x=0}} \qquad (38)$$

The transfer matrix is readily obtained by a fourth order Runge-Kutta scheme. We have experimented with other schemes and consider it quite probable that in future development some advantage, particularly in speed, may be gained by using a different integration scheme.

The propagation in the uniform ducts $x < 0$ and $x > \ell$ can be expressed in terms of the classical duct theory. In a uniform duct $u(x,y)$, $p(x,y)$, $v(x,y)$ can be written

$$\underset{3\times 1}{\begin{Bmatrix} u(x,y) \\ p(x,y) \\ v(x,y) \end{Bmatrix}} = \underset{3\times 2N}{\begin{bmatrix} c\alpha_m^+ e_m^+ \cos \bar{\kappa}_m^+ y & c\alpha_m^- e_m^- \cos \bar{\kappa}_m^- y \\ \rho_o c^2 e_m^+ \cos \bar{\kappa}_m^+ y & \rho_o c^2 e_m^- \cos \bar{\kappa}_m^- y \\ c\beta_m^+ e_m^+ \sin \bar{\kappa}_m^+ y & c\beta_m^- e_m^- \sin \bar{\kappa}_m^- y \end{bmatrix}} \underset{2N\times 1}{\begin{Bmatrix} a_m^+ \\ a_m^- \end{Bmatrix}} \qquad (39)$$

where

$$e_m^+ = e^{-ik_{x_m}^+ x} \qquad e_m^- = e^{-ik_{x_m}^- x}$$

$$\alpha_m^+ = \frac{k_{x_m}^+/k}{1 - M k_{x_m}^+/k} \qquad \alpha_m^- = \frac{k_{x_m}^-/k}{1 - M k_{x_m}^-/k}$$

$$\beta_m^+ = -i\frac{\bar{\kappa}_m^+/k}{1 - M k_{x_m}^+/k} \qquad \beta_m^- = -i\frac{\bar{\kappa}_m^-/k}{1 - M k_{x_m}^-/k}$$

$$\frac{k_{x_m}}{k} = \frac{1}{1-M^2}\left[-M \pm \sqrt{1-(1-M^2)\left(\frac{\bar{\kappa}_m}{k}\right)^2}\right]$$

The plus and minus superscripts denote right (positive) and left (negative) moving modes. The $\bar{\kappa}_m$ are the eigenvalues in the uniform duct. The determination of the direction of propagation of a given mode is discussed in Appendix B in the general case of softwall ducts. We have generally carried out our computations treating the uniform ducts as hardwalled. In this case

$$\bar{\kappa}_m^+ = \bar{\kappa}_m^- = \frac{(m-1)\pi}{b} \quad ; \qquad m = 1, 2, \cdots N$$

The choice of sign in k_{x_m}/k for positive and negative moving modes can then be deduced by energy flow arguments[13].

The nondimensional speed of sound $c = c^*/c_r$ and density $\rho_o = \rho_o^*/\rho_r$ appear because the classical duct solution used here is based on nondimensionalization with respect to the duct density and speed of sound, c^* and ρ^*. These reference conditions will generally be different in the ducts $x < 0$ and $x > \ell$. In the duct $x < 0$, $c = 1$ and $\rho_o = 1$ because we have defined c_r and ρ_r as conditions existing in the duct $x < 0$. In the duct $x > 0$ we define $c = c_F$ and $\rho_o = \rho_F$, the nondimensional speed of sound and density at the end of the nonuniformity.

The velocities and pressure in the nonuniformity can be written in matrix form

$$\underset{3\times 1}{\begin{Bmatrix} u(x,y) \\ p(x,y) \\ v(x,y) \end{Bmatrix}} = \underset{3\times 6N}{\begin{bmatrix} \underset{1\times 2N}{\cos\kappa_m y} & & \\ & \underset{1\times 2N}{\cos\kappa_m y} & \\ & & \underset{1\times 2N}{\sin\kappa_m y} \end{bmatrix}} \underset{6N\times 1}{\begin{Bmatrix} u_m \\ p_m \\ v_m \end{Bmatrix}} \tag{40}$$

The eigenvalues in the nonuniform section are ordered so that m = 1,2,...N correspond to right running modes and m = N+1, N+2,...2N correspond to left running modes. The method of obtaining the κ_m and the technique used to sort them for the direction of propagation is discussed in Appendix B in a print of a paper to appear in the Journal of Sound and Vibration.

To demonstrate the matching procedure we write Eq. (39) for x = 0 and x = ℓ in abbreviated form

$$\underset{3\times 1}{\begin{Bmatrix} u \\ p \\ v \end{Bmatrix}_{x=0}} = \underset{3\times 2N}{[K_0]} \underset{2N\times 1}{\begin{Bmatrix} a_m^+ \\ a_m^- \end{Bmatrix}} \tag{41}$$

$$\underset{3\times 1}{\begin{Bmatrix} u \\ p \\ v \end{Bmatrix}_{x=\ell}} = \underset{3\times 2N}{[K_\ell]} \underset{2N\times 1}{\begin{Bmatrix} c_m^+ \\ c_m^- \end{Bmatrix}} \tag{42}$$

As described in Reference (1), the amplitude coefficients at x = ℓ have absorbed the exponential terms $e^{-ik_{x_m}^+\ell}$, $e^{-ik_{x_m}^-\ell}$ and are thus amplitude coefficients referenced to x = ℓ, rather than x = 0. Equation (40) is written in abbreviated form at x = 0 and x = ℓ

$$\underset{3\times 1}{\begin{Bmatrix} u \\ p \\ v \end{Bmatrix}_{x=0}} = \underset{3\times 6N}{[C_0]} \underset{6N\times 1}{\begin{Bmatrix} u_m \\ p_m \\ v_m \end{Bmatrix}_{x=0}} \tag{43}$$

$$\underset{3\times 1}{\begin{Bmatrix} u \\ p \\ v \end{Bmatrix}_{x=\ell}} = \underset{3\times 6N}{[C_\ell]} \underset{6N\times 1}{\begin{Bmatrix} u_m \\ p_m \\ v_m \end{Bmatrix}_{x=\ell}} \tag{44}$$

At x = 0, we match u,p,v to obtain

$$\underset{3\times 6N}{[C_o]} \underset{6N\times 1}{\begin{Bmatrix} u_m \\ p_m \\ v_m \end{Bmatrix}_{x=\ell}} = \underset{3\times 2N}{[K_o]} \underset{2N\times 1}{\begin{Bmatrix} a_m^+ \\ a_m^- \end{Bmatrix}}$$

We use a least squares estimate for the u_m, p_m, v_m. This is obtained in the form

$$\underset{6N\times 1}{\begin{Bmatrix} u_m \\ p_m \\ v_m \end{Bmatrix}_{x=0}} = \underset{6N\times 2N}{[A(0)]} \underset{2N\times 1}{\begin{Bmatrix} a_m^+ \\ a_m^- \end{Bmatrix}} \tag{45}$$

where

$$\underset{6N\times 2N}{[A(0)]} = \underset{6N\times 6N}{[CC_o]}^{-1} \underset{6N\times 2N}{[CK_o]}$$

and

$$\underset{6N\times 6N}{[CC_o]} = \int_0^b \underset{6N\times 3}{[\tilde{C}_o]^T} \underset{3\times 6N}{[C_o]}\, dy$$

$$\underset{6N\times 2N}{[CK_o]} = \int_0^b \underset{6N\times 3}{[\tilde{C}_o]^T} \underset{3\times 2N}{[K_o]}\, dy$$

The operation $[\tilde{C}_o]^T$ denotes the complex conjugate transpose. This computation can be viewed as establishing the starting values for u_m, p_m, v_m from the wave amplitudes in the duct x < 0.

At x = ℓ, we match u, and p:

$$\underset{3\times 4N}{[C_\ell]} \underset{4N\times 1}{\begin{Bmatrix} u_m \\ p_m \end{Bmatrix}}_{x=\ell} = \underset{3\times 2N}{[K_\ell]} \underset{2N\times 1}{\begin{Bmatrix} c_m^+ \\ c_m^- \end{Bmatrix}}$$

The matrix $[C_\ell]$ is truncated to delete the 2N columns related to v_m. We again use a least squares matching to obtain

$$\underset{2N\times 1}{\begin{Bmatrix} C^+ \\ C^- \end{Bmatrix}} = \underset{2N\times 4N}{[A(\ell)]} \underset{4N\times 1}{\begin{Bmatrix} u_m \\ p_m \end{Bmatrix}}_{x=\ell} \tag{46}$$

where

$$\underset{2N\times 4N}{[A(\ell)]} = \underset{2N\times 2N}{[KK_\ell]}^{-1} \underset{2N\times 4N}{[KC_\ell]}$$

and

$$\underset{2N\times 2N}{[KK_\ell]} = \int_0^b \underset{2N\times 3}{[\tilde{K}_\ell]^T} \underset{3\times 2N}{[K_\ell]}\, dy$$

$$\underset{2N\times 4N}{[KC_\ell]} = \int_0^b \underset{2N\times 3}{[\tilde{K}_\ell]^T} \underset{3\times 4N}{[C_\ell]}\, dy$$

Again, the operation $[\tilde{K}_\ell]^T$ signifies the complex conjugate transpose. We use this notation with the general case in mind when the uniform duct is softwalled. When it is hardwalled, as generally assumed in our computations, we have dispensed with the conjugate because the eigenfunctions are orthogonal and a straight Fourier matching is possible.

This operation is viewed as determining the wave structure in the duct x > ℓ from the conditions at the end of the nonuniformity. We are considering the possibility of matching u,p,v at x = ℓ, rather than just u and p. The extra computation is insignificant and might prove beneficial since the extra information available for determining c_m^+ and c_m^- might help smooth out any inaccuracies which have been introduced in the process of developing the transfer matrix. This procedure has not as yet been implemented.

Equations (38), (45) and (46) can now be combined to yield

$$\underset{2N\times 1}{\begin{Bmatrix} C_n^+ \\ C_n^- \end{Bmatrix}} = \underset{2N\times 4N}{[A(\ell)]}\underset{4N\times 6N}{[T]}\underset{6N\times 2N}{[A(0)]}\underset{2N\times 1}{\begin{Bmatrix} a_m^+ \\ a_m^- \end{Bmatrix}}$$

$$= \underset{2N\times 2N}{[TA]}\underset{2N\times 1}{\begin{Bmatrix} a_m^+ \\ a_m^- \end{Bmatrix}} \qquad (47)$$

The matrix $[T]$ is truncated with the 2N rows corresponding to the v equations deleted.

From this point on the technique of obtaining the matrices of reflection and transmission coefficients follows Reference (1). We assume an infinite duct $x > \ell$. Then

$$\begin{Bmatrix} C_n^+ \\ 0 \end{Bmatrix} = \begin{bmatrix} TA_{11} & TA_{12} \\ TA_{21} & TA_{22} \end{bmatrix}\begin{Bmatrix} a_m^+ \\ a^- \end{Bmatrix}$$

From this we obtain

$$\{a^-\} = -[TA_{22}]^{-1}[TA_{21}]\{a^+\} = [REF]\{a^+\} \qquad (48)$$

$$\{C^+\} = \left([TA_{11}] + [TA_{12}][REF]\right)\{a^+\} = [TRAN]\{a^+\} \qquad (49)$$

where $[\mathrm{REF}]$ and $[\mathrm{TRAN}]$ are the reflection and transmission coefficient matrices, respectively. The extension to finite ducts $x > \ell$ follows the development of Reference (1).

RESULTS

As noted previously, the development of the computational scheme has gone through three stages, beginning with the use of no-flow modes for basis functions, progressing to positive running flow modes as basis functions, and then finally to the use of the complete set of flow modes as basis functions. Each stage of development represents a new level of complexity. When no-flow modes are used the formulation follows almost directly from the no-flow case described in Reference (1) with the use of a new set of governing equations, as described by Eqs. (36) of this document. In advancing to the use of the positive propagating flow modes the eigenvalue scheme of Reference (1) must be abandoned for the one described in Appendix B. Both of these implementations represent a size increase over the equivalent no-flow problem so that computational time approximately doubles. The ultimate level of complexity arises in using both positive and negative running flow modes as basis functions. Assuming that the same level of resolution is available by using basis functions of similar character this formulation leads to computational times in the neighborhood of nine times that of the original no flow case. It is apparent that a very careful evaluation with regard to accurracy and computing cost must be made to ascertain the appropriate level of complexity required to treat the problem.

The major problem faced in this program has been the almost total lack of any results against which to make comparisons and evaluation. As noted in Reference (1), we were forced to develop several alternative computational schemes to make an evaluation of the results of the no-flow computational scheme. None of the alternative schemes of the no-flow case are available to us in the flow case. The only approach we have been able to take is the reduction of the general scheme to certain special cases. Of particular interest in this regard is the computational scheme of Davis and Johnson[6] in which they treat plane wave propagation through a one dimensional compressible flow in a variable cross section duct. Their computational scheme should allow us to generate results which serve as low frequency comparisons for the computational schemes developed here.

Other comparisons that we have used serve only as gross indications of the consistency of our present formulation. We have approached zero flow speed and compared the results against our original no flow results. Since the

governing equations in the flow case don't degenerate directly to the no flow equations this type of comparison provides an independent check of some of the terms. We have also used the straight hardwalled duct as a comparison since we know that reflection coefficients should vanish and that transmission coefficients can be computed by simple hand computations. A further simple test case considers uniform soft wall ducts. In this case we are again able to compare against simple hand calculations. Finally, we have generated results for a uniform soft wall segment between two infinite hardwalled ducts. These results have been compared against similar results generated by another investigation.

In this section we will discuss our computations to date in the form of a series of comparisions as noted above. The most extensive results so far obtained are for the simplest case in which the no-flow basis functions are used. Since the use of flow mode basis functions is a recent development, only a less extensive series of results is available. In particular, as we will discuss later, the use of both positive and negative propagating modes has lead to a series of new computational problems not encountered previously. As a consequence our major effort in this case has been directed toward isolating the problems and taking corrective measures.

A. COMPUTATIONAL COMPARISONS USING NO-FLOW BASIS FUNCTIONS AND POSITIVE RUNNING FLOW BASIS FUNCTIONS

As we have indicated, the use of no-flow (NF) basis functions or positive running flow (PF) basis functions represents a large savings in computational complexity and cost in comparison to the use of the complete set of positive and negative running flow (PNF) basis functions. Numerical experimentation has been carried out to determine if the NF and PF basis functions provide satisfactory results.

The NF basis functions are certainly the simplest to use since the associated eigenvalues follow from a simple eigenvalue equation and it seems fairly certain that the functions form a complete set, each member of the set being orthogonal to the others. The completeness is essential for the Galerkin approach and the orthogonality is an advantage computationally since the coupling between modes in minimized. One form of our computational scheme uses the NF modes. As a step toward using PNF basis functions we have developed a form of the computer program which uses the PF basis functions. This formulation is not much more complicated than when the NF basis functions are used, except that the associated eigenvalue equation is more difficult to use.

The basis functions in this case are not orthogonal and we observe more coupling between the modes. Of particular concern is the completeness of the set of basis functions. Since the PF basis functions are a subset of the PNF modes, they may not themselves be complete. At the current stage of development our only means of ascertaining their usefulness in numerical experimentation. This experimentation has been done in the following test cases:

(a) Convergence of results at low Mach numbers to results obtained with the original no-flow duct program.
(b) Convergence to the straight hardwall duct case in which hand calculations can be made.
(c) Convergence to the straight uniform softwalled duct case in which hand calculations can be made.
(d) Comparison of results of several schemes for softwalled, straight segment between two hardwalled, infinite ducts.
(e) Comparison against a one dimensional, low frequency approximation.

The following sub-sections describe the comparisons made to date.

(a) Convergence to no flow case

As reported in Reference (1), the computational scheme applicable when no mean flow is present has been highly successful and provides a convenient base-line against which to check the results of the present program. When flow is present the governing equations, as given by Eqs. (36), are not computationally the same as the no flow case, even when the flow Mach number becomes small. To be made computationally the same a number of reductions and substitutions would have to be made. However, we have found that by making computations in the flow case at low Mach numbers we have been able to duplicate the no flow results. As an example, we have considered a linearly tapered, softwall transition section between two uniform hardwalled ducts. We have considered a wall admittance of $A = 0.413 + i\ 0.720$, a taper ratio of $b_\ell/b_0 = 1.268$, a reduced frequency $kb_0 = 1.5$, $\ell = 1.0$ and $b_0 = 1.0$. In Table 1 results are compared using the no flow program and the flow program with NF and PF modes. Using the PF modes we were forced to use $M = 0.05$ to avoid severe numerical problems which arise when the general equations are run at very low Mach number. This comes up because the leading terms in the v_n differential equations tend to vanish. This didn't occur using NF modes, but we feel that it is at least partly due to the difference in precision we used on the IBM 360 for the NF modes and the Burroughs B6718 we used for the PF modes. In addition, for expedience, we used 80 integration steps and 3 modes in the PF case and used 100 steps and 5 modes in the NF case. Near zero Mach number the stability and accuracy of the integration is sensitive to the number of steps. Even with this difference in

Mach number we see that the results are definitely tending toward the no-flow results. These results support the accuracy of the terms in the general equations which are not flow related. They do not support a particular choice of basis functions because at small Mach numbers the NF and PF modes are nearly the same.

(b) Convergence to the Hardwall case

The computation of the transmission in a hardwall uniform duct provides a means to determine the accuracy of the uniform flow terms in the equations. To this end we have considered a high Mach number, M = -0.8, a nearly hardwall, A = 0.0001 + i 0.0001, at kb = 1.0, with $b_0 = b_\ell = 1.0$ and $\ell = 1.0$. Both NF and PF modes were used. Table 2 is a comparison of results obtained analytically and results obtained from the knowledge that in a uniform duct no reflection or spurious mode generation occurs. The diagonal transmission terms are obtained by noting that for right moving waves the pressure solution is given by

$$P_n = A_n e^{-i k_{x_n}^+ x} \psi_n(y)$$

The ratio of pressures at x = ℓ and x = 0 is

$$TRAN_{nn} = e^{-i k_{x_n}^+ \ell}$$

For the case at hand

$$k_{x_n}^+ = \frac{k}{1-M^2}\left[-M \pm \sqrt{1-(1-M^2)\left(\frac{\kappa_n}{k}\right)^2}\right]$$

where

$$\frac{\kappa_n}{k} = \frac{(n-1)\pi}{kb} \qquad n = 1, 2,$$

The positive sign applies for n = 1 and the negative sign for n > 1. Using the parameters given we obtain

$k_{x_1}^+ = 5.0 + i\,0.0$ $\qquad TRAN_{11} = -0.8391 + i\,0.5440$

$k_{x_2}^+ = 2.222 - i\,4.4384$ $\qquad TRAN_{22} = -0.0000 + i\,0.0001$

It is seen that these calculated results agree almost exactly with the results obtained computationally. Once again, this test case offers no insight into the choice of modes since in the hardwall case the NF and PF modes are the same.

(c) Convergence to the Uniform Softwall Duct Case

Transmission in a uniform softwall duct is also easily obtained by hand calculation and provides a convenient check case. Due to the particular formulation of our program we are only able to do this for the PF basis functions. We have considered the case M = -0.5, kb = 1.0, A = 0.720 + i 0.420, $b_0 = b_\ell = 1.0$, $\ell = 1.0$. The calculated results, obtained as in subsection (b), except with k_x defined from the computer program, are as follows:

$k_{x_1}^+ = 1.5237 - \iota\, 1.0108$ $\qquad$ $TRAN_{11} = 0.0171 - \iota\, 0.3636$

$k_{x_2}^+ = 0.6787 - \iota\, 4.5384$ $\qquad$ $TRAN_{22} = 0.0083 - \iota\, 0.0067$

We have used 3 modes in the computational scheme and in this formulation essentially bypass the matching procedure which becomes unnecessary. Table 3 shows the results of the comparison and indicates complete agreement.

This check case does not verify the completeness of the PF modes simply because correct results are obtained. The PF modes are individually exact solutions to this problem. We are not asking them to produce a solution to a new problem.

(d) Convergence to a Softwall, Uniform Segment Between Two Hardwall Infinite Ducts

A somewhat more challenging problem from a computational point of view arises when we consider a uniform softwall segment between two infinite hardwall ducts. The solution in the lined segment is exactly the same as obtained in the problem discussed in Sub-section (c). However, in this case we are matching the solution to hardwall ducts rather than infinite softwall ducts.

Since reflection and spurious mode generation can occur we can observe the performance of the NF and PF modes, that is, we can observe if the solution in the lined section provides enough detail to predict the more complex acoustic field. To this end we have made two comparisons, one at low Mach number and one at high Mach number.

In the low Mach number case we have used M = -0.1, A = 0.72 + i 0.42, kb = 1.0, $b_0 = b_\ell = 1.0, \ell = 1.0$. In table 4 we have compared transmission and reflection coefficients using NF and PF modes with results from a mode matching scheme due to J.F. Unruh of the Boeing Co., Seattle, Washington. Because of the differences in the implementation of the mode matching scheme, only two reflection and transmission coefficients are directly comparable to our results. It is noted that the results of all three methods are nearly the same. At low Mach numbers the NF modes and the PF modes are not greatly different (they are identical at no-flow conditions), so it is not totally surprising that they yield similar results. It is significant that the results compare well with the mode matching approach, which is completely independent.

As a second check case we have used M = -0.50, A = 0.720 + i 0.42, kb = 1.0, $b_0 = b_\ell = 1.0$, $\ell = 1.0$. We have again compared the current program using NF and PF modes with mode matching results. The results of this comparison are given in Table 5. We notice a definite degradation in the comparison between the solution using the NF modes and the mode matching although the trends compare well. As we did not generate the mode matching results we can only assume their correctness at this point. Accepting this assumption, we feel that the degradation is due to the fact that the NF modes are not close solutions to the problem which involves flow, and hence it probably requires an increased number of basis functions to generate accurate results as compared to the no-flow case. The results using the PF basis functions are seen to be totally off. In Subsection (c) we used these basis functions to generate results for exactly the same conditions with the exception of the matching to uniform hard wall ducts as in the present case. In Subsection (c) we obtained very good results, compared to exact hand calculations. Since the solution in the"non-uniform segment" is the same in both cases, it follows that the poor correlation in the present case arises because of the matching. This indicates that the solution in the non-uniformity is not detailed enough to account for reflection and spurious mode generation. The original thought that the PF basis functions are not complete, and hence can't stand on their own as a

series expansion for the softwall case, seems to be borne out.

In order to more fully verify the trends when the NF modes are used, we need to develop an independent mode matching capability. The majority of the building blocks are available, but the press of other program development has prevented putting it together.

(e) Comparison With a One Dimensional Formulation

Davis and Johnson[6] have developed a one dimensional model of acoustic transmission through a compressible flow in a nonuniform hard walled duct. We have adapted this formulation to treat problems of the type encountered in the present investigation. The approach is to substitute an integration of their governing differential equation for the transfer matrix integration scheme in the program we have developed. The matching of the nonuniform segment to infinite uniform ducts is done in essentially the same way as explained previously. The Davis and Johnson (DJ) formulation can be considered a low frequency approximation, since only at low frequencies can we be assured of primarily plane wave propagation, as assumed in their analysis.

To generate comparisons with the general program we have considered inlet (flow opposite to propagation) and exhaust (flow and propagation directions coincide) cases for a duct with a cosine shaped converging taper. In the DJ formulation the walls are hard and in the general formulation we take $A = 0.0001 + i\ 0.0001$. The reduced frequency is $kb_0 = 1.0$, with $b_0 = 1.0$, $b_\ell = 0.75$ and $\ell = 2.0$. Mach numbers at $x = 0$ in the range $-0.5<M_0<0.5$ are considered. These corresponded to Mach numbers at $x = \ell$ in the range $-0.93<M<0.93$. In the general program we have made the majority of our calculations using the NF modes but we have made runs using the PF basis functions at selected Mach numbers. Figures 2 and 3 show the comparison of results. The original NF results show good agreement with the DJ results for transmission coefficients for the entire Mach number range. Reflection coefficients show reasonable agreement in exhaust flows, but diverge from the one dimensional results for high inlet Mach numbers. The introduction of the PF modes has made a major improvement at high inlet Mach numbers and agreement is good, particularly for the reflection coefficient. We notice

some deviation in the transmission coefficient at M = -0.5, but in the light of the approximation in the MJ method this is not considered significant. At this point the improvement is not thought to be due to the PF modes, which with hard walls should be the same as NF modes, but rather because of an improved implementation of the matching procedure at the ends of the nonuniformity. We consider this correlation to be of major significance in supporting the validity of the MWR.

B. COMPUTATIONAL COMPARISONS USING COMPLETE FLOW BASIS FUNCTIONS

To attempt to overcome certain shortcomings in the NF and PF basis function form of the Method of Weighted residuals, we have developed a form of the program utilizing the PNF basis functions. As noted previously, this form of the program is costly in terms of computer time and storage, but must be considered potentially more accurate because the basis functions are more nearly solutions to the problem, containing information on both positive and negative running modes. The PNF basis functions are probably complete, but they are not orthogonal, which creates coupling between the modes.

In developing the PNF basis function formulation we encountered numerical problems which did not airse in our previous developments. In integrating the set of differential equations of Eqs. (37) to obtain the transfer matrix $[T]$, definied in Eq. (38), it was found that if the nonuniform duct segment is long (e.g. $\ell = b_0$), then elements of the transfer matrix are large enough to make the subsequent matching operations numerically inaccurate. While this problem can be at least partially overcome by increased precision in the computations, it indicates a sensitivity that was not previously seen in equivalent cases in the original no flow problem or in the NF and PF formulations. We have circumvented the problem by considering only short segments (e.g. $\ell = 0.1\, b_0$). This means that the analysis of a long duct will require the solution of a series of short duct segments and then a stepped matching procedure. In this situation we have essentially developed an acoustic finite element for a duct segment. We consider this to be an acceptable utilization of the method. We have also found the PNF case to be much more sensitive at low Mach numbers to the trend toward the breakdown in the form of the differential equations caused by the duct mean flow

velocity approaching zero.

A second major problem which has been noted is due to the use of both positive and negative running flow modes. The matrices $[N_{nm}]$ and $[M_{nm}]$ whose elements are defined by

$$N_{nm} = \int_0^b \psi_n \psi_m \, dy$$

$$M_{nm} = \int_0^b \phi_n \phi_m \, dy$$

are apparently very nearly singular. We find numerically that the inverse of the leading matrix in Eq.(36) generates very large numbers (although our inverse scheme is known to produce an accurate inverse) which subsequently must be operated on through matrix multiplication on the right hand side to generate more moderately sized numbers. It is felt that this is a potential numerical trouble spot and the implications should be more carefully assessed. This appears to be telling us that even when the duct is soft walled and the flow does not vanish, the PNF basis functions are nearly linearly dependent. It may thus turn out that the right running modes and the left running modes are not sufficiently independent to perform well computationally. We hope to be able to explore the implications of this observation in more detail. At the present time we are exercising caution in maintaining a double check on computational aspects such as the accuracy of inverses.

In order to provide an indication of the correctness of the PNF program we have made several runs against cases which have a simple analytic solution. These check cases are:

(a) Convergence to uniform hard wall duct results.

(b) Convergence to uniform soft wall duct results.

Table 6 shows the comparison of the hardwall duct results using PNF modes against the exact solution. We have used M = -0.5, kb = 1.0, $b_0 = b_\ell = 1.0$, A = 0.0001 + i 0.0001, and $\ell = 0.10$. The analytical results are generated as in Subsection (b) of Section A. They yield

$k_{x_1}^+ = 2.0 + i\,0.0$ $\qquad$ $TRAN_{11} = 0.9801 - i\,0.1987$

$k_{x_2}^+ = 0.6667 - i\,3.374$ $\qquad$ $TRAN_{22} = 0.7120 - i\,0.0475$

As shown in the table the computed and analytical results compare nearly exactly.

Table 7 is a similar comparison using results for a uniform softwall duct. In this case we have used M = -0.5, kb = 5.0, $b_0 = b_\ell = 1.0$, A = 0.720+i0.420, and ℓ = 0.10. The analytical results yield

$$k_{x_1}^+ = 9.7343 - i\,0.02995 \qquad TRAN_{11} = 0.5608 - i\,0.8243$$

$$k_{x_2}^+ = 6.9892 - i\,0.6915 \qquad TRAN_{22} = 0.7142 - i\,0.6003$$

The comparison is seen to be very good.

These comparisons, though limited in scope tend to support the implementation of the PNF version of the Method of Weighted residuals. Because of the numerical problems that we have been forced to overcome we have not as yet mechanized the procedure by which we build up the solution for long ducts by mode matching the solutions for a series of shorter duct elements. This has prevented us from making the most demanding comparison against the Davis and Johnson low frequency, plane wave formulation.

At the present time we feel that the PNF formulation is in basically good order. Check cases have been favorable and work is continuing toward implementing the mode matching technique. Sufficient experience has been gained to observe that the PNF form of the method of weighted residuals is computationally demanding and costly in terms of storage and run time. We are still working toward the point where the relative merits of PNF can be compared against the NF and PF implementations.

CONCLUSIONS AND EXTENSIONS

The Method of Weighted Residuals in the form of a modified Galerkin method with weighted boundary residuals has been shown to be an accurate and efficient method for the analysis of the propagation of sound in nonuniform ducts with no flow. The method has been extended to include problems of propagation in ducts carrying a steady compressible mean flow. This extension must still be considered in the development stage in which extensive numerical experimentation is being carried out to optimize the implementation. Three different schemes are currently operational. These schemes differ in the type of basis functions used, the simplest implementation using modes from uniform ducts with no flow (NF), the other two using positive running nodes,including the flow effect (PF) and positive and negative running flow modes (PNF).

The greatest amount of experience has been obtained with the NF basis functions. We have found that these modes yield good results over a wide Mach number range when compared against a simpler theory for low frequency propagation through a one dimensional flow in a hard wall, variable area duct. The method, as implemented,appears to break down at high inlet Mach numbers for calculation of the reflection coefficient. Results for transmission coefficient hold up through the entire subsonic range. Other check cases involving convergence to certain limiting cases of lined ducts have been generally good at low Mach numbers with degradation as Mach number increases (based on the presumption of accurate baseline results from other sources). This is not unexpected since for ducts with soft walls the NF modes become increasingly poor approximations to actual solutions as the Mach number increases, and we expect to require a large number of basis functions to sythesize a solution.

The results with the PF basis functions have been mixed. In the hard wall, variable area duct our PF implementation gives good results over the entire Mach number range. This represents an improvement over the NF implementation. Since for hard walls the NF and PF modes ought to coincide, we currently feel that it is the implementation of the NF modes which the PF program has improved on. The improvement is most likely in the matching procedure. In soft wall ducts the PF modes are apparently not adequate. They fail in the limiting problem of a straight, lined section between two infinite hardwall ducts. It is felt that lack of completeness may be the problem. These modes are an exact solution in the lined segment. However, the transfer matrix generated when they are used is not detailed enough to account for reflected and spurious modes which arise due to the impedance discontinuity. Numerical

experimentation with PF modes is still in progress.

The development of a computational scheme employing PNF modes introduces new computational problems not previously encountered. The problems have been identified and are due to the rapid growth in dimensionality caused by the doubling of the number of modes and the coupling between modes due to the lack of orthogonality of the modes. At the present time the technique for overcoming these difficulties is to consider only short duct segments, on the the order of 1/10 of the duct height. This restriction does not render the MWR impractical, since longer nonuniformites can be treated by breaking the duct down into short sub-sections which can then be put together using mode matching techniques. When used in this context each sub-section can be viewed as an acoustic finite element. Because of the extensive development and analysis required in the PNF case we have only a limited computational experience. The comparison of results using PNF modes with certain limiting cases have been favorable. However, as noted elsewhere, computational costs rise rapidly because of the increased dimensionality. At the present time this implementation is still being developed and will be continued.

We have accumulated sufficient experience with the three approaches to develop a strong preference for the use of the NF basis functions. This preference is based on the absence of severe numerical difficulties, the relative simplicity of the implementation and the relative expense when compared to the other two possibilities. It is believed that the problem noted in comparing to the Davis-Johnson one dimensional results can be eliminated so that the NF program will work as well as the PF program for this type of problem. However, we still recognize certain inadequacies. The most notable one is the apparent trend away from correlation with mode matching results as Mach number increases in the test case of a soft wall segment between infinite hard wall ducts. Our future research will be directed toward an improved form of the NF program. This will include a detailed analysis of the computations to identify problem areas. We currently favour a modification of the basis functions which may lead to an improvement in performance. It has been observed that the principal effect of flow on the basis functions is to change the lower modes, but leave the higher modes fairly close to the no-flow modes. It seems possible that a set of basis functions using the lowest two or three PNF modes and the higher NF modes will improve the potential accuracy of the NF method. Of course we can't make an assessment of the completeness of this choice of basis functions without experimentation.

As part of our future development we plan to write a simple mode matching

program to generate results as a baseline for comparison in our straight duct convergence studies. We have previously used results generated by other investigators, but we would prefer to develop independent results.

Finally, in both the no flow and flow programs we have noticed a trend toward numerical difficulties if the basis functions include modes deep into cut-off. This problem is most severe when we are dealing with low reduced frequencies, since in this case it may require a number of cut-off modes to provide enough resolution to obtain a converged solution by the Galerkin method. We feel that it is the exponential character of the cut-off solutions that creates the difficulty. To alleviate this we currently have under development a modification of the computational scheme which essentially explicitly isolates this exponential behaviour so that the transfer matrix is not required to include it. This modification is nearly complete and if successful will be reported in the open literature.

REFERENCES

1. W. Eversman, E.L. Cook, and R.J. Beckemeyer 1974 Journal of Sound and Vibration 37(3), 105-123. A method of weighted residuals for the investigation of sound transmission in non-uniform ducts without flow.

2. A. Powell 1960 Journal of the Acoustical Society of America 32, 1640-1646. Theory of sound propagation through ducts carrying high speed flow.

3. N.A. Eisenberg and T.W. Kao 1969 Journal of the Acoustical Society of America 49, 169-175. Propagation of sound through a variable area duct with a steady compressible flow.

4. L.S. King and K. Karamcheti, 1973 Proceedings of the American Institute of Aeronautics and Astronautics Aero-Acoustics Conference, Seattle, Washington, October 15-17, Paper 73-1009. Propagation of plane waves in the flow through a variable area duct.

5. P. Huerre and K. Karamcheti 1973 Proceedings of Interagency Symposium on University Research in Transportation Noise, Stanford University, March 28-30. Propagation of sound through a fluid moving in a duct of varying area.

6. S.S. Davis and M.L. Johnson 1974 87th Meeting of the Acoustical Society of America, New York, April 23-26, Paper KK-2. Propagation of plane waves in a variable area duct carrying a compressible subsonic flow.

7. C.K.W. Tam 1971 Journal of Sound and Vibration 18, 339-351. Transmission of spinning acoustic modes in a slightly non-uniform duct.

8. A.H. Nayfeh, D.P. Telionis and S.G. Lekoudis 1973 Proceedings of the American Institute of Aeronautics and Astronautics Aero-Acoustics Conference, Seattle, Washington, October 15-17, Paper 73-1008. Acoustic propagation in ducts with varying cross sections and sheared mean flow.

9. C.K.W. Tam 1971 Journal of Sound and Vibration 16(3), 393-405. On finite amplitude spinning acoustic modes and subsonic choking.

10. B.A. Finlayson 1972 The Method of Weighted Residuals and Variational Principles. Academic Press.

11. B.T. Zinn and E.A. Powell 1968 Proceedings of the XIX International Astronautical Congress, Vol. 3., 59-73. Application of the Galerkin method in the solution of combustion-instability problems.

12. E.A. Powell and B.T. Zinn 1969 Israel Journal of Technology 7(1-2), 79-89. Solution of linear combustion instability problems using the Galerkin method.

13. W Eversman 1971 Journal of the Acoustical Society of America 49, 1717-1721. The transmission of acoustic energy in a duct with flow.

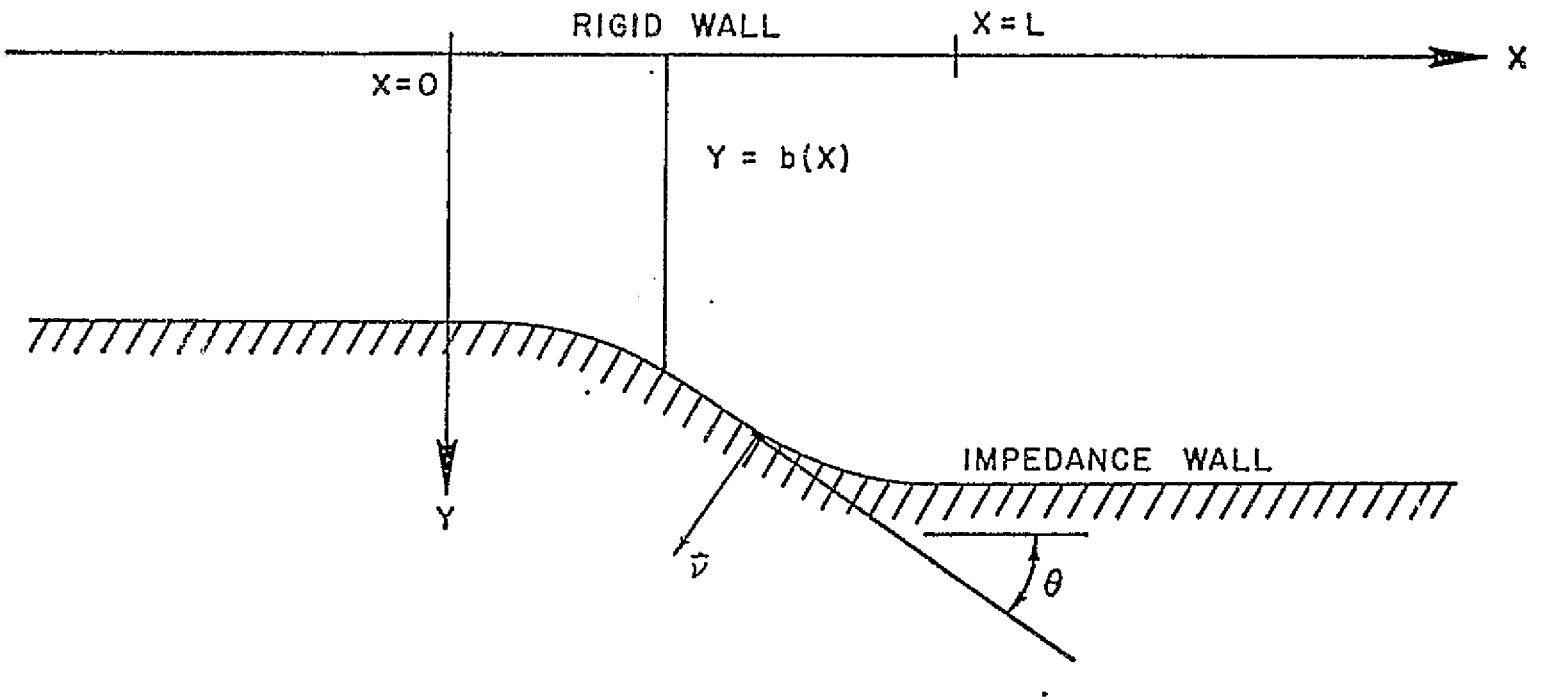

FIGURE I
DUCT GEOMETRY FOR EXAMPLE CASE

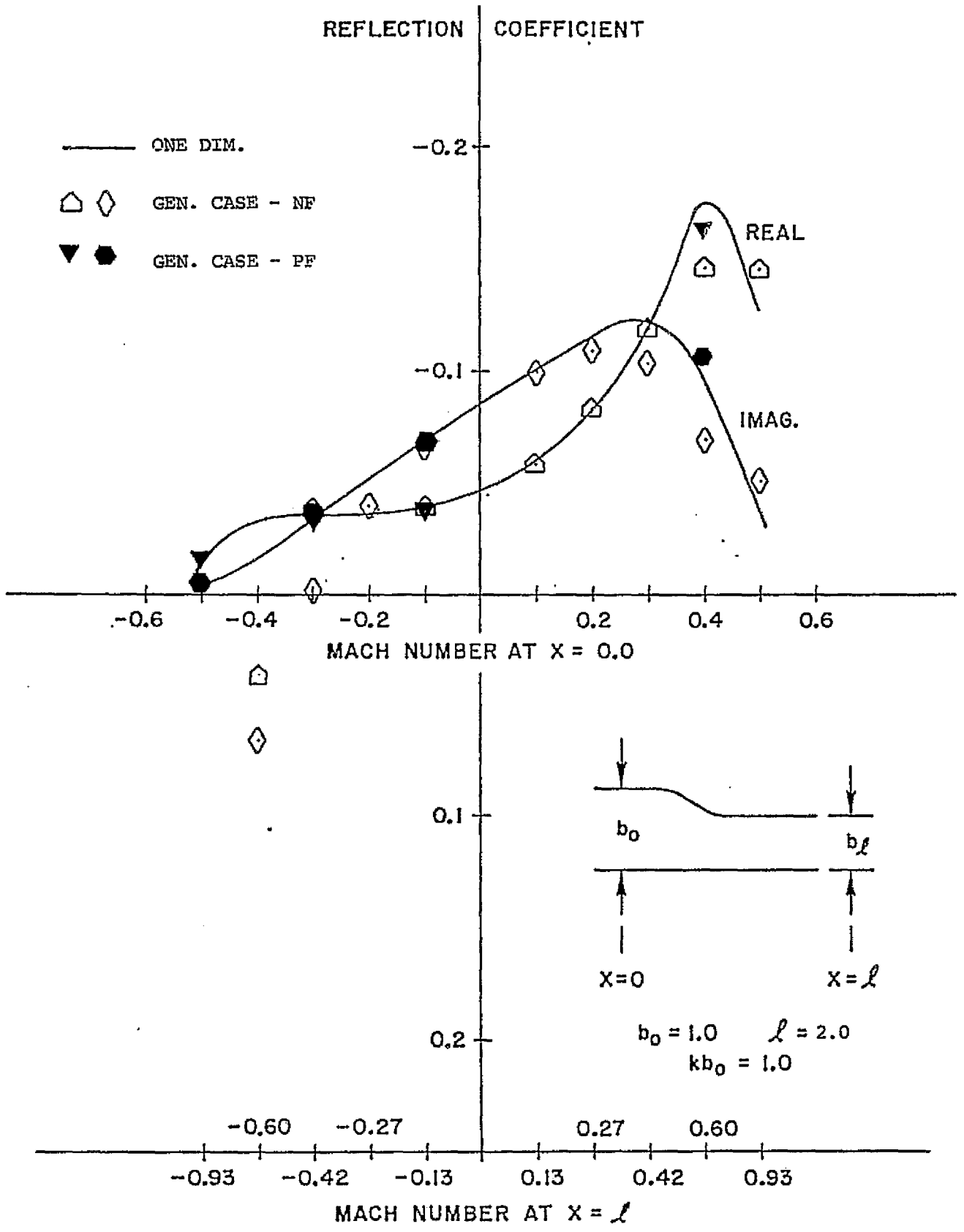
COSINE TAPER ~ $b_\ell / b_0 = 0.75$
REFLECTION COEFFICIENT
ONE DIM.
GEN. CASE - NF
GEN. CASE - PF
REAL
IMAG.
-0.2
-0.1
0.1
0.2
-0.6
-0.4
-0.2
0.2
0.4
0.6
MACH NUMBER AT X = 0.0
b_0
b_ℓ
X=0
$X=\ell$
$b_0 = 1.0$ $\ell = 2.0$
$kb_0 = 1.0$
-0.60
-0.27
0.27
0.60
-0.93
-0.42
-0.13
0.13
0.42
0.93
MACH NUMBER AT $X = \ell$

Figure 2

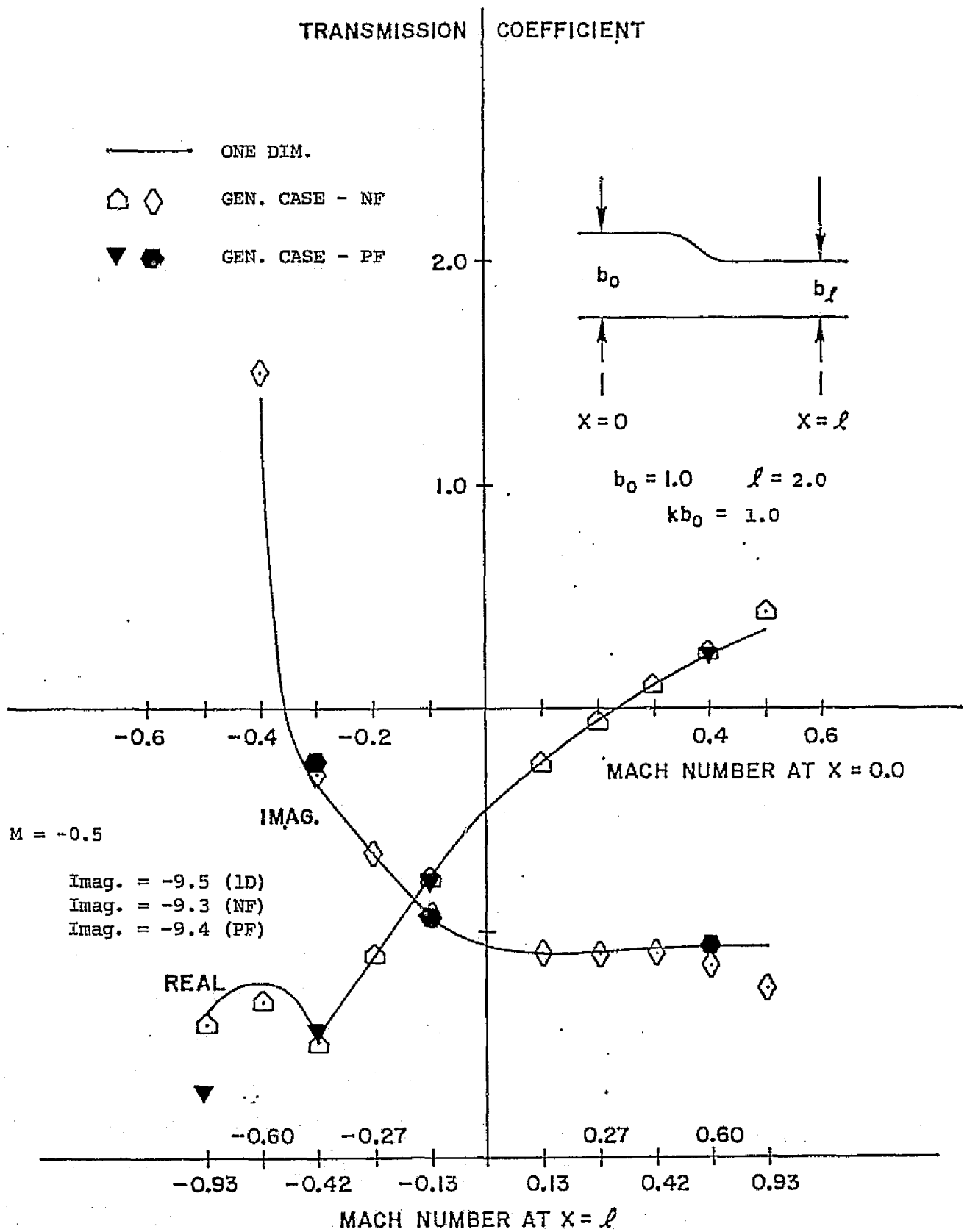
COSINE TAPER ~ $b_\ell / b_0 = 0.75$
TRANSMISSION COEFFICIENT
ONE DIM.
GEN. CASE - NF
GEN. CASE - PF
2.0
1.0
b_0
b_ℓ
X = 0
X = ℓ
b_0 = 1.0 ℓ = 2.0
kb_0 = 1.0
-0.6 -0.4 -0.2 0.4 0.6
MACH NUMBER AT X = 0.0
IMAG.
M = -0.5
Imag. = -9.5 (1D)
Imag. = -9.3 (NF)
Imag. = -9.4 (PF)
REAL
-0.60 -0.27 0.27 0.60
-0.93 -0.42 -0.13 0.13 0.42 0.93
MACH NUMBER AT X = ℓ

Figure 3

Table 1

CONVERGENCE OF FLOW CASE TO NO FLOW CASE

$kb_0 = 1.5$ Linear Taper $b_i/b_0 = 1.268$ $A = 0.413 + i\ 0.72$

$\ell = 1.0$ $b_0 = 1.0$

M=0.01 - NF Modes

REFLECTION COEFFICIENTS

	1	2
1	-0.0776+i0.2539	0.1431+i0.0004
2	0.0040+i0.1522	0.0340-i0.0563

TRANSMISSION COEFFICIENTS

	1	2
1	-0.1628-i0.6314	0.0965-i0.0073
2	0.1586+i0.1949	0.1165-i0.0326

M=0.05 - PF Modes

REFLECTION COEFFICIENTS

	1	2
1	-0.0742+i0.2593	0.1504+i0.0036
2	0.0175+i0.1476	0.0303-i0.0584

TRANSMISSION COEFFICIENTS

	1	2
1	-0.1148-i0.6711	0.0978+i0.0069
2	0.1372+i0.2082	0.1221-i0.0309

No Flow

REFLECTION COEFFICIENTS

	1	2
1	-0.0785+i0.2524	0.1420-i0.0008
2	0.0009+0.1544	0.0343-i0.0563

TRANSMISSION COEFFICIENTS

	1	2
1	-0.1741-i0.6197	0.0960-i0.0111
2	0.1644+i0.1910	0.1151-i0.0332

Table 2

CONVERGENCE TO STRAIGHT HARD WALL DUCT

$kb = 1.0 \quad b_\ell/b_0 = 1.0 \quad A = 0.0001+i0.0001, \; b_0 = 1.0 \quad \ell = 2.0$

M=-0.8 - NF Modes

EFLECTION COEFFICIENTS

1	2
0.0000+i0.0000	0.0000-i0.0000
-0.0003+i0.0002	0.0001-i0.0001

RANSMISSION COEFFICIENTS

-0.8357+i0.5446	-0.0003+i0.0000
-0.0001-i0.0004	-0.0000+i0.0001

M=-0.8 - PF Modes

REFLECTION COEFFICIENTS

	1	2
1	0.0000+i0.0000	0.0000+i0.0000
2	0.0000+i0.0000	0.0000+i0.0000

TRANSMISSION COEFFICIENTS

1	-0.8357+i0.5445	0.0000+i0.0000
2	0.0000+i0.0000	0.0000+i0.0000

M=-0.8 - Calculated

REFLECTION COEFFICIENTS

	1	2
1	0.0000+i0.0000	0.0000+i0.0000
2	0.0000+i0.0000	0.0000+i0.0000

TRANSMISSION COEFFICIENTS

1	-0.8391+i0.5440	0.0000+i0.0000
2	0.0000+i0.0000	-0.0000+i0.0000

Table 3

CONVERGENCE TO UNIFORM STRAIGHT DUCT

$kb = 1.0 \quad b_\ell/b_0 = 1.0 \quad A = 0.72+i0.42 \quad b_0 = 1.0 \quad \ell = 1.0$

M=-0.50 PF Modes

REFLECTION COEFFICIENTS

	1	2
1	0.0+i0.0	0.0+i0.0
2	0.0+i0.0	0.0+i0.0

TRANSMISSION COEFFICIENTS

	1	2
1	0.0171-i0.3635	0.0003-i0.0001
2	0.0000+i0.0000	0.0081-i0.0069

M=-0.50 - Calculated

REFLECTION COEFFICIENTS

	1	2
1	0.0+i0.0	0.0+i0.0
2	0.0 i0.0	0.0+i0.0

TRANSMISSION COEFFICIENTS

	1	2
1	0.0171-i0.3636	0.0+i0.0
2	0.0+i0.0	0.0083-i0.0067

Table 4

STRAIGHT SOFT WALL SEGMENT BETWEEN HARDWALL INFINITE DUCTS

kb = 1.0 b_ℓ/b_0 A = 0.72+i0.42 b_0 = 1.0 ℓ = 1.0

M=-0.1 - NF Modes

REFLECTION COEFFICIENTS

	1
1	-0.195+i0.167
2	-0.030+i0.080

TRANSMISSION COEFFICIENTS

	1
1	0.187-i0.588
2	0.057+i0.042

M=-0.1 - PF Modes

REFLECTION COEFFICIENTS

	1
1	-0.1967+i0.167
2	-0.0287+i0.0806

TRANSMISSION COEFFICIENTS

	1
1	0.1873-i0.5882
2	0.05712+i0.0433

M=-0.1 - Mode Matching

REFLECTION COEFFICIENTS

	1
1	-0.1922+i0.170
2	-0.028+i0.079

TRANSMISSION COEFFICIENTS

	1
1	0.190-i0.587
2	0.059+i0.0421

Table 5

STRAIGHT SOFTWALL SEGMENT BETWEEN HARDWALL INFINITE DUCTS

$kb = 1.0 \quad b_\ell/b_0 = 1.0 \quad A = 0.72+i0.42 \quad b_0 = 1.0 \quad \ell = 1.0$

M=-0.5 - NF Modes

REFLECTION COEFFICIENTS

	1
1	-0.1074+i0.2030
2	-0.0631+i0.2742

TRANSMISSION COEFFICIENTS

	1
1	0.0220-i0.3353
2	0.0696-i0.0751

M=-0.5 PF Modes

REFLECTION COEFFICIENTS

	1
1	- 0.0798+i0.3583
2	0.0104+i0.1480

TRANSMISSION COEFFICIENTS

	1
1	0.0083-i0.1211
2	0.1590-i0.2104

M=-0.5 - Mode Matching

REFLECTION COEFFICIENTS

	1
1	-0.077+i0.1665
2	-0.091+i0.2126

TRANSMISSION COEFFICIENTS

	1
1	-0.0103-i0.3646
2	0.057-i0.084

Table 6

CONVERGENCE TO UNIFORM HARD WALL DUCT

$kb = 1.0 \quad b_\ell/b_0 = 1.0 \quad A = 0.0001+i0.0001 \quad b_0 = 1.0 \quad \ell = 0.1$

M=-0.5 - PNF Modes

REFLECTION COEFFICIENTS

	1	2
1	0.0002+i0.0000	0.0000+i0.0000
2	0.0000+i0.0000	0.0000+i0.0000

TRANSMISSION COEFFICIENTS

	1	2
1	0.9798-i0.1988	0.0000+i0.0000
2	0.0000+i0.0000	0.7120-i0.04755

M=-0.5 - Calculated

REFLECTION COEFFICIENTS

	1	2
1	0.0+i0.0	0.0+i0.0
2	0.0+i0.0	0.0+i0.0

TRANSMISSION COEFFICIENTS

	1	2
1	0.9801-i0.1987	0.0+i0.0
2	0.0+i0.0	0.7120-i0.04753

Table 7

CONVERGENCE TO STRAIGHT SOFT WALL DUCT

$kb = 5.0 \quad b_\ell/b_0 = 1.0 \quad A = 0.720+i0.420 \quad b_0 = 1.0 \quad \ell = 0.10$

M=-0.5 - PNF Modes

REFLECTION COEFFICIENTS

	1	2
1	0.0000+i0.0000	0.0002+i0.0000
2	0.0000+i0.0000	0.0000-i0.0003

TRANSMISSION COEFFICIENTS

	1	2
1	0.5608-i0.8243	0.0002+i0.0002
2	0.0000+i0.0000	0.7144-i0.6004

M=-0.5 - Calculated

REFLECTION COEFFICIENTS

	1	2
1	0.0+i0.0	0.0+i0.0
2	0.0+i0.0	0.0+i0.0

TRANSMISSION COEFFICIENTS

	1	2
1	0.5608-i0.8243	0.0+i0.0
2	0.0+i0.0	0.7142-i0.6003

Appendix A

REPRODUCTION OF REFERENCE (1)

JSV—MS 186—Slip 473
327-10/11 + 1 pt—9thqr set—32em—39.7 own—8-9-74—

704059
BLG

Journal of Sound and Vibration (1974) 37(3), 000-000

A METHOD OF WEIGHTED RESIDUALS FOR THE INVESTIGATION OF SOUND TRANSMISSION IN NON-UNIFORM DUCTS WITHOUT FLOW

W. Eversman and E. L. Cook

Wichita State University, Wichita, Kansas 67208, *U.S.A.*

AND

R. J. Beckemeyer

The Boeing Company, Wichita, Kansas 67210, *U.S.A.*

(*Received* 30 *May* 1974, *and in revised form* 18 *July* 1974)

The transmission of sound in a non-uniform two dimensional duct without flow is investigated by a method of weighted residuals which leads to a set of coupled "generalized telegraphists' equations". Results for several duct configurations are compared with those from, respectively, a variational method, a stepped duct approximation, and an eigenfunction expansion method based on linearly tapered duct segments.

1. INTRODUCTION

Relatively rigorous methods have been developed for the analysis and design of acoustically lined and unlined ducts of uniform rectangular, circular, and annular cross section, with and without flow, and including the boundary layer effect in the flow case. The progress in this area can be seen by referring to a few papers of the extensive literature which exists (see, for example, references [1]–[5]). The current capability in the mathematical modeling of duct propagation is limited primarily by the assumption of a uniform, infinite duct.

There have been a few recent studies directed toward the non-uniform duct problem. In the case of ducts without flow a generally useful approach is the one developed by Zorumski and Clark [6] for ducts of uniform area with lining variations and subsequently implemented by Alfredson [7] for the study of hard-walled ducts with varying cross section. This method consists of representing the duct by a series of stepped ducts of uniform cross-section and systematically accounting for the reflection and transmission process which occurs at the intersection of the stepped elements. This procedure appears to be very useful provided it is used with due caution in the segmenting process. In the case of ducts with uniform area but varying lining properties, it has been shown by Bahar [8], for the case of electromagnetic waveguides, to converge to the method developed in the present paper when the elemental segments become vanishingly short. The principal difficulty with the stepped duct approach as originally conceived is the high dimensionality of the numerical problem which results. A somewhat different formulation of the problem by the third author of the present paper has reduced this difficulty while retaining the flexibility of the method.

Another method of general utility for ducts without flow is the variational approach of Beckemeyer and Eversman [9]. In this technique the acoustic problem is represented by a variational principle and a Ritz minimization is employed to determine the coefficients in a trial solution. The trial solution is in terms of basis functions which do not necessarily satisfy the boundary conditions (the boundary conditions are part of the functional in the variational formulation) and do not have to be generated for each duct geometry. The stepped duct

approach requires a set of eigenfunctions and eigenvalues in each stepped section and in the case of lined ducts this can be a problem in terms of computational requirements (the method introduced in the present paper must have eigenvalues and eigenfunctions at stations along the duct, but, as will be described, a rapid numerical scheme has been devised for their computation). The variational approach suffers a dimensionality problem in that complicated acoustic fields (both axial and transverse) require a large number of basis functions in the trial solution.

Other recent approaches to the problem are more approximate in nature by virtue of restricting geometry or frequency range allowed. Nayfeh and his co-workers have published several studies of propagation in non-uniform ducts with and without flow. The paper by Nayfeh, Telionis and Lekoudis [10] is representative. They restrict themselves to ducts with slowly varying cross-section, lining properties and flow properties and employ a perturbation scheme. To within the level of accuracy which they retain, they do not predict the generation, reflection, and transmission of modes other than the one incident on the non-uniformity. It appears that a higher level of approximation is required to predict this.

Karamcheti and his co-workers have also made contributions in this area. King and Karamcheti [11] studied plane waves in ducts with one dimensional flow by a method of characteristics and Huerre and Karamcheti [12] used a short wave approximation for the same type of problem. Similar problems were studied earlier by Powell [13] and Eisenberg and Kao [14].

Tam [15] seems to have published the first paper dealing with a multi-modal approach to the problem of non-uniform ducts with flow. His technique is a perturbation scheme based on the assumption of slowly varying cross-sectional area. The first order approximate solution is obtained by Fourier transformation.

A recent paper by Cummings [16] studies the novel problem of the acoustics of a wine bottle. The wine bottle is a non-uniform duct without flow and the acoustic field is approximated by a Runge–Kutta integration scheme based on the Webster Horn Equation. This method allows only a plane wave mode of propagation and hence is limited to the lower frequency ranges. There have been many studies of the horn equation since Rayleigh first introduced it and it is a favorite topic in texts on acoustics.

In the present research program we are interested in the multi-modal propagation of sound in non-uniform ducts of fairly general shape. The final goal of the program is the study of propagation in non-uniform ducts with flow, so that we will be interested in methods for the no flow case which appear to be extendable to the case with flow. Of the two generally applicable techniques mentioned previously, the variational method does not seem to be readily extendable to the case with flow. The stepped duct approximation might have some application, although it is certainly questionable whether the non-uniform flow field can be represented in sufficient detail in a series of stepped uniform segments. We are thus led to look for another method with promise for the flow case. In this paper we will introduce the method and assess its utility in the case without flow, as there are equivalent results available against which a direct comparison can be made. In the course of the development and application of the method it has become apparent that the method of weighted residuals is an important alternate method for the duct with no flow, and indeed, may well be superior to the other two methods of general utility.

The method of weighted residuals (MWR) employed here actually was first employed in connection with electromagnetic waveguide problems by Schelkunoff [17, 18]. The field equations for these problems are identical to the classical acoustic equations in certain cases. Schelkunoff's work followed work by Stevenson [19, 20] which used MSR but led to a somewhat different formulation which does not seem to have been widely used. Stevenson appears to be the first to suggest the application of methods of this type to acoustic horn problems.

Bahar and his co-workers studying ionospheric propagation of microwaves as a terrestrial waveguide problem have made extensive use of MWR (see, for example, reference [8]) and Reiter [21] has formalized the approach.

In this paper we have used MWR to approach the problem of multi-modal propagation in non-uniform ducts without flow. We deal with a two dimensional duct in which both area variations and lining variations are permitted. The results obtained by using MWR are compared with those, respectively, from a stepped duct theory, the variational approach, and a segmented duct theory in which the duct segments are radial (sectoral). In reviewing the literature it does not appear that results for lined ducts of variable cross-section in the multi-modal case, with fairly general area variations permitted, have previously been presented.

2. METHOD

In this analysis two dimensional ducts of infinite length are considered. The extension to circular, annular, or rectangular ducts is straightforward, but of course more demanding computationally. The extension to include finite duct terminations is easily included in the present formulation provided reflection and transmission characteristics of the termination are available.

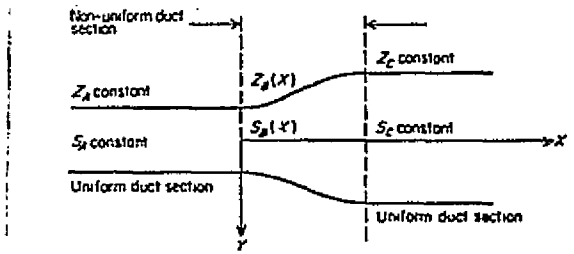

Figure 1. Duct configuration.

Figure 1 shows the type of configuration under consideration, in which two semi-infinite uniform duct sections of wall impedance z_a and z_c and areas s_a and s_c are joined by a transition section of length l of variable area $s_b(x)$ and variable impedance $z_b(x)$, where x is the axial co-ordinate. In this analysis the area variation will be restricted to be continuous, but the lining variation can be discontinuous at the ends of the non-uniformity.

In terms of dimensional acoustic pressure, p^*, particle velocity, $\mathbf{V}^*$, and density, ρ^*, the acoustic equations for complex harmonic motion of the form $e^{i\omega t}$ in time are

$$i\omega p^* + \rho_0 \operatorname{div} \mathbf{V}^* = 0,$$
$$i\omega \rho_0 \mathbf{V}^* = -\operatorname{grad} p^*,$$
$$p^* = c^2 \rho^*,$$

where the ambient state is given by p_0, ρ_0, $\mathbf{V}_0 = 0$ and $c = (\gamma p_0/\rho_0)^{1/2}$ is the ambient speed of sound. By introducing the non-dimensional variables $p = p^*/\rho_0 c^2$, $\rho = \rho^*/\rho_0$, $\mathbf{V} = \mathbf{V}^*/c$ and eliminating ρ one can write

$$ikp + \operatorname{div} \mathbf{V} = 0 \tag{1}$$

$$ik\mathbf{V} = -\operatorname{grad} p \tag{2}$$

where $k = \omega/c = 2\pi/\lambda$ and λ is the free space wave number.

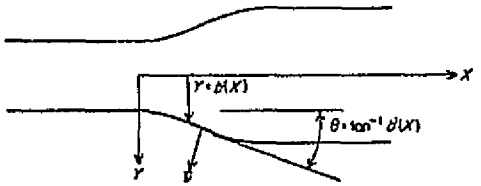

Figure 2. Duct co-ordinate system.

In order to specify a boundary condition at the duct walls, a co-ordinate system as shown in Figure 2 is introduced. This figure shows the manner in which the duct height profile and slope of the height profile are specified as well as the designation of the local outward unit normal at the duct wall, ν. The duct wall boundary condition employed is characteristic of a normally reacting lining in the presence of a harmonic pressure variation: namely,

$$p^* = zV_\nu^* = z\mathbf{V}^* \cdot \nu, \tag{3}$$

where V_ν^* is the component of the acoustic particle velocity in the direction of the outward normal. z is the wall impedance which may be a function of axialposition. In non-dimensional variables equation (3) becomes

$$p = \frac{z}{\rho_0 c}\mathbf{V} \cdot \nu,$$

or

$$\mathbf{V} \cdot \nu = Ap, \tag{4}$$

at the duct wall, where $A = \rho_0 c/z$ is the acoustic admittance ratio of the lining. In the case of a uniform duct of two dimensional, circular, annular, or rectangular cross section equations (1), (2) and (4) can be combined to produce the classical problem of propagation in a lined duct which has been thoroughly studied. In these problems powerful techniques can be brought to bear since a co-ordinate geometry can be chosen to make both the field equations and the boundary conditions variables separable. For general non-uniform ducts this is not possible and an alternate approach must be used.

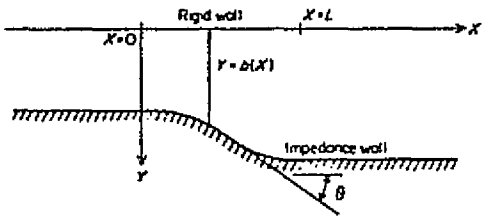

Figure 3. Duct geometry for example problems.

To demonstrate the method of weighted residuals (see Finlayson's book [22] for a complete description of the general method), we consider a two dimensional duct as shown in Figure 3 in which the wall at $y = 0$ is hard and the wall at $y = b(x)$ is lined with a material of admittance $A(x)$. This representation is also valid for a duct symmetric about the x-axis with the acoustic propagation also symmetric with this axis. The governing equations are

equations (1) and (2) with the boundary condition obtained by expanding equation (4):

$$v = 0, \qquad y = 0, \tag{5}$$

$$v\cos\theta - u\sin\theta = Ap, \qquad y = b(x), \tag{6}$$

where u and v are the non-dimensional axial and transverse velocity components and $\tan\theta = db/dx$ is the wall slope.

We seek solutions to this problem in the form of a finite series of specified basis functions:

$$p_N = \sum_{n=1}^{N} p_n(x)\cos\kappa_n y, \tag{7}$$

$$u_N = \sum_{n=1}^{N} u_n(x)\cos\kappa_n y, \tag{8}$$

$$v_N = \sum_{n=1}^{N} v_n(x)\sin\kappa_n y, \tag{9}$$

where the κ_n are defined as the infinite sequence of eigenvalues of

$$\kappa b\tan\kappa b = ikbA.$$

The basis functions are recognized as the eigenfunctions for propagation in a uniform duct which has the same height and admittance as the non-uniform duct has locally. This means that the eigenvalues κ_n are functions of x and that the basis functions change with axial position. Note that these basis functions do not individually satisfy the boundary condition of equation (6); however MWR will force them to do so collectively. The choice of basis functions may seem to be unnecessarily complicated since we will be required to provide a new set of eigenvalues and eigenfunctions at each axial position; however, we will show that this can be done quickly and easily. Any disadvantage is outweighed by the more rapid convergence of this type of technique when the basis functions are chosen to represent as nearly as is practical the actual solution.

If the trial solutions, equations (7)–(9), are substituted in the differential equations and boundary conditions, they do not in general satisfy them, but instead leave an error, or residual. Thus, in terms of these trial solutions one can write

$$R_1 = ikp_N + \frac{\partial u_N}{\partial x} + \frac{\partial v_N}{\partial x},$$

$$R_2 = iku_N + \frac{\partial p_N}{\partial x},$$

$$R_3 = ikv_N + \frac{\partial p_N}{\partial y},$$

$$R_4 = (v_N\cos\theta - u_N\sin\theta - Ap_N)_{y=b}.$$

Since a continuous function must be zero if it is orthogonal to every member of a complete set we will force these residuals to be orthogonal to every member of the complete set formed

by the basis functions themselves at every station x along the duct axis:

$$\int_0^b R_1(x,y)\cos\kappa_n y\,dy = 0, \tag{10}$$

$$\int_0^b R_2(x,y)\cos\kappa_n y\,dy = 0, \tag{11}$$

$$\int_0^b R_3(x,y)\sin\kappa_n y\,dy = 0, \tag{12}$$

$$R_4(x,b)\cos\kappa_n b = 0. \tag{13}$$

The operations indicated by equations (10)–(13) yield, for $\xi = 1, 2, \ldots N$,

$$ik\int_0^b p_N\cos\kappa_n y\,dy + \int_0^b \frac{\partial u_N}{\partial x}\cos\kappa_n y\,dy + \int_0^b \frac{\partial v_N}{\partial y}\cos\kappa_n y\,dy = 0, \tag{14}$$

$$ik\int_0^b u_N\cos\kappa_n y\,dy + \int_0^b \frac{\partial p_N}{\partial x}\cos\kappa_n y\,dy = 0, \tag{15}$$

$$ik\int_0^b v_N\sin\kappa_n y\,dy + \int_0^b \frac{\partial p_N}{\partial y}\sin\kappa_n y\,dy = 0, \tag{16}$$

$$(v_N\cos\theta - u_N\sin\theta - Ap_N)\cos\kappa_n b = 0. \tag{17}$$

By using Leibnitz's rule for differentiation of integrals containing a parameter the partial derivatives of u_N and p_N with respect to x in equations (14) and (15) can be replaced by ordinary derivatives. For example:

$$\int_0^b \frac{\partial u_N}{\partial x}\cos\kappa_n y\,dy = \frac{d}{dx}\int_0^b u_N\cos\kappa_n y\,dy - \int_0^b u_N\frac{\partial}{\partial x}[\cos\kappa_n y]\,dy - u_N(x,b)\cos\kappa_n b\frac{db}{dx}$$

The partial derivatives with respect to y can be eliminated by integration by parts:

$$\int_0^b \frac{\partial v_N}{\partial y}\cos\kappa_n y\,dy = v_N(x,b)\cos\kappa_n b + \kappa_n\int_0^b v_N\sin\kappa_n y\,dy,$$

$$\int_0^b \frac{\partial p_N}{\partial y}\sin\kappa_n y\,dy = p_N(x,b)\sin\kappa_n b - \kappa_n\int_0^b p_N\cos\kappa_n y\,dy. \tag{18}$$

Equation (16) can be used to eliminate v_n from equation (14) and the boundary residual, equation (17), is used to simplify the boundary terms in the resulting equation. In this way,

equations (14) through (17) can be written in terms of two equations:

$$\frac{d}{dx}\int_0^b u_N\cos\kappa_n y\,dy = -ik\left[1-\left(\frac{\kappa_n}{k}\right)^2\right]\int_0^b p_N\cos\kappa_n y\,dy + \int_0^b u_N\frac{\partial}{\partial x}(\cos\kappa_n y)\,dy - \\ -i\left[\kappa_n b\tan\kappa_n b - \frac{ikbA}{\cos\theta}\right]\frac{p_N(x,b)\cos\kappa_n b}{kb}, \tag{19}$$

$$\frac{d}{dx}\int_0^b p_N\cos\kappa_n y\,dy = -ik\int_0^b u_N\cos\kappa_n y\,dy + \int_0^b p_N\frac{\partial}{\partial x}(\cos\kappa_n y)\,dy + p_N(x,b)\cos\kappa_n b\frac{db}{dx}. \tag{20}$$

The trial solutions for p_N and u_N are substituted into equations (19) and (20). In the case of the duct without flow the eigenfunctions are orthogonal so that

$$\int_0^b \cos\kappa_n y\cos\kappa_m y\,dy = N_n\delta_{nm},$$

where $\delta_{nm} = 0$, $\xi \neq m$, and $\delta_{nn} = 1$.

Equations (19) and (20) become

$$\frac{du_n}{dx} = -ik\left[1-\left(\frac{\kappa_n}{k}\right)^2\right]p_n - \sum_{m=1}^{N} U_{nm}^u u_m - \sum_{m=1}^{N} U_{nm}^p p_m, \tag{21}$$

$$\frac{dp_n}{dx} = -iku_n - \sum_{m=1}^{N} P_{nm}^p p_m, n = 1, 2, \ldots N, \tag{22}$$

where

$$U_{nm}^u = \frac{1}{N_n}\frac{dN_n}{dx}\delta_{nm} + \frac{1}{N_n}\frac{d\kappa_n}{dx}\int_0^{Hm^2} y\sin\kappa_n y\cos\kappa_m y\,dy,$$

$$U_{nm}^p = i\left[b_n\tan\kappa_n b - \frac{ikbA}{\cos\theta}\right]\frac{\cos\kappa_n b\cos\kappa_m b}{N_n kb},$$

$$P_{nm}^p = U_{nm}^u - \frac{\tan\theta}{N_n}\cos\kappa_n b\cos\kappa_m b.$$

Equations (21) and (22) can be represented in matrix form by

$$\left\{\begin{array}{c}\frac{du_n}{dx}\\ \hline \frac{dp_n}{dx}\end{array}\right\} = \left[\begin{array}{c|c}-[U_{nm}^u] & -\left[ik\left(1-\left(\frac{\kappa_n}{k}\right)^2\right)\delta_{nm}\right]-[U_{nm}^p] \\ \hline -[ik\delta_{nm}] & -[P_{nm}^p]\end{array}\right]\left\{\begin{array}{c}u_m\\ \hline p_m\end{array}\right\}. \tag{23}$$

It is noted that if the duct is uniform so that $d\kappa_n/dx = 0$ and $db/dx = \tan\theta = 0$ then equations (21) and (22) reduce to equations for the axial field in a uniform duct corresponding to each mode of propagation. In this case they are a form of the telegraphists' equations. When the

duct is non-uniform, coupling terms are introduced and the resulting equations are "generalized telegraphists' equations", a term introduced by Schelkunoff [17].

Equations (21) and (22), or their equivalent matrix form in equation (23), will define the acoustic field in the non-uniformity providing one can specify initial and or final conditions on the u_n and p_n at the start of the non-uniformity at $x = 0$ and the end $x = l$. This can be done by assuming that the sound is incident from the left, or $x < 0$, and the acoustic field for $x < 0$ consists of incident and reflected waves. For $x > l$, in this analysis, we assume the sound propagates to the right in a semi-infinite uniform duct, and hence consists only of waves propagating away from the non-uniformity. In general, one can write, for $x < 0$,

$$u(x,y) = \sum_n \left(\frac{\bar{k}_n}{k}\right)[a_n^+ e^{-i\bar{k}_n x} - a_n^- e^{i\bar{k}_n x}]\cos\bar{\kappa}_n y,$$

$$p(x,y) = \sum_n [a_n^+ e^{-i\bar{k}_n x} + a_n^- e^{i\bar{k}_n x}]\cos\bar{\kappa}_n y,$$

where a_n^+, a_n^- are coefficients of the incident and reflected waves, respectively. $\bar{\kappa}_n$ are the eigenvalues for propagation in the uniform duct for $x < 0$, and

$$\frac{\bar{k}_n}{k} = \pm\sqrt{1 - \left(\frac{\bar{\kappa}_n}{k}\right)^2},$$

where the plus sign is chosen if $\bar{k}_n/k$ is real and if $\bar{k}_n/k$ is complex the sign is chosen to make the imaginary part negative. One can write similar expressions for the uniform duct, $x > l$:

$$u(x,y) = \sum_n \left(\frac{k_n^*}{k}\right)[b_n^+ e^{-ik_n^* x} - b_n^- e^{ik_n^* x}]\cos\kappa_n^* y,$$

$$p(x,y) = \sum_n [b_n^+ e^{-ik_n^* x} + b_n^- e^{ik_n^* x}]\cos\kappa_n^* y,$$

where the starred quantities apply for $x > l$. At $x = 0$ one can match particle velocity and pressure:

$$\sum_n \left(\frac{\bar{k}_n}{k}\right)[a_n^+ - a_n^-]\cos\bar{\kappa}_n y = \sum_n u_n \cos\kappa_n y,$$

$$\sum_n [a_n^+ + a_n^-]\cos\bar{\kappa}_n y = \sum_n p_n \cos\kappa_n y.$$

If the same number of uniform duct eigenfunctions as there are basis functions in the non-uniformity is used, then the orthogonality of the eigenfunctions can be used to obtain a matrix relation between the a_n^+ and a_n^- and the u_n and p_n at $x = 0$. This is

$$\left[\begin{array}{c:c} \alpha_{mn} & \\ \hdashline & \alpha_{mn} \end{array}\right]\left\{\begin{array}{c} u_m(0) \\ \hdashline p_m(0) \end{array}\right\} = \left[\begin{array}{c:c} \left(\frac{\bar{k}_m}{k}\right)\bar{\alpha}_{mn} & -\left(\frac{\bar{k}_m}{k}\right)\bar{\alpha}_{mn} \\ \hdashline \bar{\alpha}_{mn} & \bar{\alpha}_{mn} \end{array}\right]\left\{\begin{array}{c} a_m^+ \\ \hdashline a_m^- \end{array}\right\}, \tag{24a}$$

where, at $x = 0$

$$\alpha_{mn} = \int_0^{b_0} \cos\kappa_n y \cos\kappa_m y\,dy = N_n \delta_{mn},$$

$$\bar{\alpha}_{mn} = \int_0^{b_0} \cos\kappa_n y \cos\bar{\kappa}_m y\,dy.$$

An exactly analogous relationship can be obtained at $x = l$:

$$\left[\begin{array}{c:c} \beta_{mn} & \\ \hdashline & \beta_{mn} \end{array}\right]\left\{\begin{array}{c} u_m(l) \\ \hdashline p_m(l) \end{array}\right\} = \left[\begin{array}{c:c} \left(\frac{k_m^*}{k}\right)\beta_{mn}^* & -\left(\frac{k_m^*}{k}\right)\beta_{mn}^* \\ \hdashline \beta_{mn}^* & \beta_{mn}^* \end{array}\right]\left[\begin{array}{c:c} c_{mn}^+ & \\ \hdashline & c_{mn}^- \end{array}\right]\left\{\begin{array}{c} b_m^+ \\ \hdashline b_m^- \end{array}\right\}, \tag{24b}$$

where, at $x = l$,

$$\beta_{mn} = \int_0^{b_l} \cos\kappa_n y \cos\kappa_m y\,dy = N_n \delta_{mn},$$

$$\beta_{mn}^* = \int_0^{b_l} \cos\kappa_n y \cos\kappa_m^* y\,dy,$$

$$c_{mn}^+ = e^{-ik_m^* l}\delta_{mn},$$

$$c_{mn}^- = e^{ik_m^* l}\delta_{mn}.$$

Hence, it is possible to obtain relations between the wave amplitudes in the uniform ducts and the pressures and particle velocities in the non-uniform section in the form

$$\begin{Bmatrix} u(0) \\ p(0) \end{Bmatrix} = [A(0)]\begin{Bmatrix} a^+ \\ a^- \end{Bmatrix}. \tag{25}$$

$$\begin{Bmatrix} u(l) \\ p(l) \end{Bmatrix} = [A(l)]\begin{Bmatrix} b^+ \\ b^- \end{Bmatrix}. \tag{26}$$

By using an integration scheme such as a fourth order Runge–Kutta, equation (23) can be integrated from $x = 0$ to $x = l$ to obtain a transfer matrix relating u_n, p_n at $x = l$ to u_n and p_n at $x = 0$:

$$\begin{Bmatrix} u(l) \\ p(l) \end{Bmatrix} = [T]\begin{Bmatrix} u(0) \\ p(0) \end{Bmatrix}. \tag{27}$$

By using equations (25) and (26), the wave amplitudes for $x > l$ can be related to those for $x < 0$:

$$\begin{Bmatrix} b^+ \\ b^- \end{Bmatrix} = [A(l)]^{-1}[T][A(0)]\begin{Bmatrix} a^+ \\ a^- \end{Bmatrix}.$$

or

$$\begin{Bmatrix} b^+ \\ b^- \end{Bmatrix} = [TA] \begin{Bmatrix} a^+ \\ a^- \end{Bmatrix}. \tag{28}$$

In the present analysis we specify that the uniform duct for $x > l$ is semi-infinite so that no reflected waves exist: i.e., $b_n^- = 0$. This enables one to write

$$\begin{Bmatrix} b^+ \\ \hline 0 \end{Bmatrix} = \left[\begin{array}{c:c} TA_{11} & TA_{12} \\ \hdashline TA_{21} & TA_{22} \end{array}\right] \begin{Bmatrix} a^+ \\ \hline a^- \end{Bmatrix}. \tag{29}$$

From equation (29) one can compute reflected and transmitted amplitudes in terms of incident amplitudes:

$$\{a^-\} = [TA_{22}]^{-1}[TA_{21}]\{a^+\},$$

$$\{b^+\} = ([TA_{11}] - [TA_{12}][TA_{22}]^{-1}[TA_{21}])\{a^+\}.$$

Thus one can define matrices of reflection coefficients and transmission coefficients:

$$[REF] = -[TA_{22}]^{-1}[TA_{21}], \tag{30}$$

$$[TRAN] = [TA_{11}] - [TA_{12}][TA_{22}]^{-1}[TA_{21}]. \tag{31}$$

The physical significance of the elements of these matrices is as follows:

REF_{ij} = Amplitude of reflected mode i due to incident mode j with amplitude $1{\cdot}0 + i0{\cdot}0$.
$TRAN_{ij}$ = Amplitude of transmitted mode i due to incident mode j with amplitude $1{\cdot}0 + i0{\cdot}0$.

In the formulation in the preceding equations we have referenced both reflected and transmitted waves with respect to $x = 0$. Because of large exponential factors which can occur for cut-off modes in the e^{-}_{mn} terms in equation (24), it appears to be more appropriate to reference the transmission coefficients to $x = l$. In this case, one can rewrite equation (24):

$$\left[\begin{array}{c:c} \beta_{mn} & \\ \hdashline & \beta_{mn} \end{array}\right] \begin{Bmatrix} u(l) \\ \hline p(l) \end{Bmatrix} = \left[\begin{array}{c:c} \left(\frac{k_{mn}^*}{k}\right)\beta_{mn}^* & -\left(\frac{k_{mn}^*}{k}\right)\beta_{mn}^* \\ \hdashline \beta_{mn}^* & \beta_{mn}^* \end{array}\right] \begin{Bmatrix} c^+ \\ \hline c^- \end{Bmatrix},$$

where

$$\begin{Bmatrix} c^+ \\ \hline c^- \end{Bmatrix} = \left[\begin{array}{c:c} c_{mn}^+ & \\ \hdashline & c_{mn}^- \end{array}\right] \begin{Bmatrix} b^+ \\ \hline b^- \end{Bmatrix}.$$

All of the steps leading to equations (30) and (31) can be repeated and a new set of reflection coefficients and transmission coefficients can be derived. The reflection coefficients will not change but the transmission coefficients referenced to $x = l$ will be related to those at $x = 0$ by

$$[TRAN]_{x=0} = [e_{mn}^-][TRAN]_{x=l}.$$

Once the reflection coefficients are obtained, one can write the initial values for $u_n(x)$ and $p_n(x)$:

$$\begin{Bmatrix} u(0) \\ p(0) \end{Bmatrix} = [A(0)] \begin{bmatrix} [I] \\ [REF] \end{bmatrix} \{a^+\}. \tag{32}$$

If the pressures and particle velocities in the non-uniformity are required, equation (23) can be integrated with equation (32) being used as initial conditions. In our computations we have stopped with the reflection and transmission coefficients for the non-uniformity, principally due to the extra computational time implied to obtain the complete acoustic field.

One can also easily account for termination conditions for $x > l$ other than the semi-infinite duct employed in this analysis. If a relationship is known between b_n^+ and b_n^- at the end of a finite uniform duct, i.e.,

$$\{b^-\} = [R]\{b^+\},$$

where $[R]$ is the termination reflection matrix, then equation (29) can be written as

$$\begin{bmatrix} [I] \\ [R] \end{bmatrix} \{b^+\} = \left[\begin{array}{c:c} TA_{11} & TA_{12} \\ \hdashline TA_{21} & TA_{22} \end{array}\right] \begin{Bmatrix} a^+ \\ \hline a^- \end{Bmatrix}.$$

Then

$$\{b^+\} = [TA_{11}]\{a^+\} + [TA_{12}]\{a^-\},$$

$$[R]\{b^+\} = [TA_{21}]\{a^+\} + [TA_{22}]\{a^-\}$$

and

$$\{a^-\} = -([R][TA_{12}] - [TA_{22}]^{-1}([R][TA_{11}] - [TA_{21}])\{a^+\},$$

$$\{b^+\} = ([TA_{11}] - [TA_{12}]([R][TA_{12}] - [TA_{22}])^{-1}([R][TA_{11}] - [TA_{21}])\{a^+\}.$$

3. IMPLEMENTATION OF THE METHOD

The most serious potential disadvantage of this form of MWR is the need to compute the eigenvalues which appear in the basis functions and hence in the coefficients in equation (23). As noted earlier the eigenvalues, κ_n, are roots of

$$\kappa b \tan \kappa b = ikbA. \tag{33}$$

The usual technique for obtaining the eigenvalues is a Newton–Raphson iteration based on suitable initial guesses. We expect to require 5 to 10 basis functions to obtain solutions sufficiently converged for our purposes, and hence we will require 5 to 10 eigenvalues for each point required in the integration scheme used to generate the transfer matrix. The iteration scheme is likely to be too costly computationally to be of practical value. We have

circumvented the problem by replacing equation (33) by the differential equation which it satisfies:

$$\frac{\mathrm{d}}{\mathrm{d}x}(2\kappa b) = \frac{1+\cos(2\kappa b)}{2\kappa b+\sin(2\kappa b)}\,2ikbA\left(\frac{1}{b}\frac{\mathrm{d}b}{\mathrm{d}x}+\frac{1}{A}\frac{\mathrm{d}A}{\mathrm{d}x}\right). \tag{34}$$

We start with values of κb at $x = 0$, for each basis function required, and generate the required values of κb at each integration step of equation (23) using a Runge–Kutta integration of equation (34). Our scheme is configured to start with no initial guess other than hard-wall eigenvalues for each required basis function at $x = 0$. This approach has proven to be far more rapid than iteration and has shown good accuracy as can be checked by occasionally evaluating Equation (32) and noting the size of the residuals which develop.

The coefficients which appear in equation (23) have previously been given. The specific terms in these coefficients are given below:

$$N_n = \frac{b}{2}\left(\frac{2\kappa_n b+\sin 2\kappa_n b}{2\kappa_n b}\right),$$

$$\frac{\mathrm{d}N_n}{\mathrm{d}x} = \frac{1}{b}\frac{\mathrm{d}b}{\mathrm{d}x}N_n - b\frac{\sin 2\kappa_n b - 2\kappa_n b\cos 2\kappa_n b}{(2\kappa_n b)^2}\frac{\mathrm{d}\kappa_n b}{\mathrm{d}x},$$

$$\int_0^b y\sin\kappa_n y\cos\kappa_m y\,\mathrm{d}y = \frac{1}{2}\left[\frac{\sin(\kappa_n-\kappa_m)b}{(\kappa_n-\kappa_m)^2}+\frac{\sin(\kappa_n+\kappa_m)b}{(\kappa_n+\kappa_m)^2}\right] - \frac{b}{2}\left[\frac{\cos(\kappa_n-\kappa_m)b}{(\kappa_n-\kappa_m)}+\frac{\cos(\kappa_n+\kappa_m)b}{(\kappa_n+\kappa_m)}\right],\quad n\neq m,$$

$$\int_0^b y\sin\kappa_n y\cos\kappa_n y\,\mathrm{d}y = \frac{b^2}{2}\left[\frac{\sin 2\kappa_n b}{(2\kappa_n b)^2}-\frac{\cos 2\kappa_n b}{2\kappa_n b}\right],\quad n = m,$$

$$\mathrm{i}\left[\kappa_n b\tan\kappa_n b-\frac{ikbA}{\cos\theta}\right]\frac{\cos\kappa_n b\cos\kappa_m b}{N_n kb} = \left(\frac{1}{\cos\theta}-1\right)\frac{\cos\kappa_n b\cos\kappa_m b}{N_n}A$$

These expressions, together with equation (33) are used to generate U^p_{nm}, U^m_{nm}, and P^p_{nm}.

4. RESULTS

Very few results have been published for the multi-modal transmission of sound in non-uniform ducts. The work of Zorumski and Clark [6], a sequel by Lansing and Zorumski [23], and the work of Alfredson [7] are the most nearly equivalent to the present method. They used the stepped duct approach for segmented linings or area changes in ducts with an open end. Since we have concentrated on the non-uniformity and have chosen not to represent terminations, we have no common basis for comparison. The approximate theories mentioned previously are considered too limited in scope to make comparison feasible when the labor and expense of doing so is considered. The only extensive results which we have been able to use conveniently are those of Beckemeyer and Eversman [9] who developed a variational approach and compared it with stepped duct approximations and an approximation in which the duct was segmented into linearly tapered sections. Of course, that study was closely related to the present one and the thrust of the entire research program has been to develop a basis of comparison.

As a first example we consider linearly tapered hard-wall transition sections joining two uniform ducts. For these cases a 15° taper transition is used. The first example is a diverging taper from a duct of height b_0 to one of height $(1+\tan 15°)b_0$, the length of the non-uniformity being equal to its initial height. The second example is a converging taper which is exactly the reverse of the diverging one. We have compared these results with those generated in reference [9] and reproduced here as Figures 4–7. In the diverging case kb_0 values of 1·0, 2·0, 2·5, 3·0 and 3·5 are compared and in the converging case kb_1 values of 1·0, 1·5, 2·0, 2·5, 3·0 are used. At $kb = 2{\cdot}5$ in the small duct the second mode is just cutting on in the large duct while at $kb = 3{\cdot}5$ in the small duct it is cut on throughout. The results from reference [9] for the diverging taper include those from two levels of stepped duct approximation (5 sections and 10 sections having been used, respectively), from the variational approach, and from a segmented duct theory (eigenfunction expansion) in which a linearly tapered duct segment with solutions given in terms of Bessel functions was used. In the last method pressures and velocities were matched at the ends of the taper, $x = 0$ and $x = l$, by collocation. No account was taken of the slight difference between the planar co-ordinate surface at the ends of the uniform duct and the circular co-ordinate surfaces of the radial segment. Details of the characteristics of these methods can be found in reference [9]. In the converging taper only the 5 section stepped duct and the variational approach were used. The MWR was used with 6 basis functions and 50 integration steps axially.

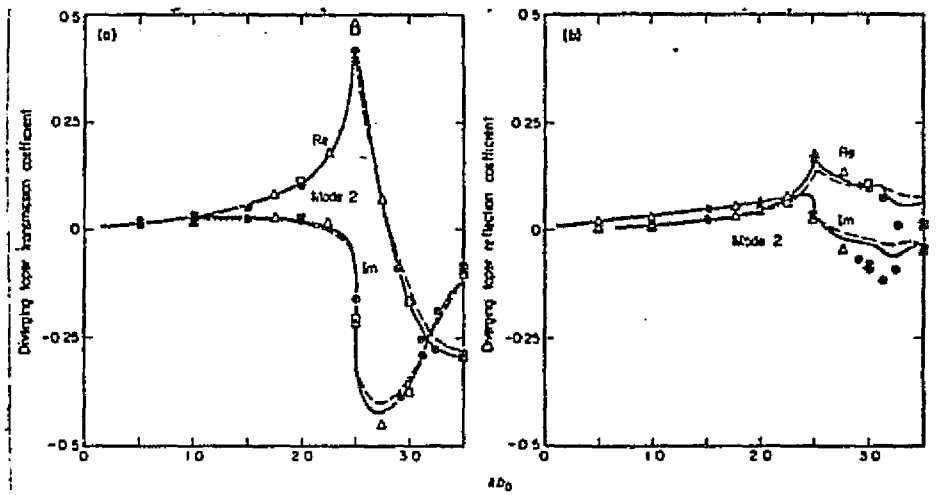

Figure 4. (a) Transmission coefficient and (b) reflection coefficient for mode 2 with mode 1 incident. Diverging 15° linearly tapered unlined transition section. $b_1 = 1{\cdot}27\ b_0$. $\alpha = 15°$; $L = b_0$. ——, 10 Section stepped duct; – – – –, 5 section stepped duct; ●, Fourier bases; △, eigenfunction expansion; □, weighted residuals.

Figures 4(a) and 5(b) show the transmission and reflection coefficients for the diverging duct for the second mode with the first mode incident at $x = 0$ with amplitude 1·0 + 0·0i. We have made the most detailed comparisons for the second mode since with increasing reduced frequency it goes through the cut-on phenomenon and hence is considered the most challenging computationally. The transmission coefficients, shown in Figure 4(a), are in good agreement throughout the frequency range, all methods considered yielding essentially the same result. In Figure 4(b), it is seen that the results for the reflection coefficients for $kb_0 > 2{\cdot}5$ are not in as good agreement. However, it is noted that the variational method, the

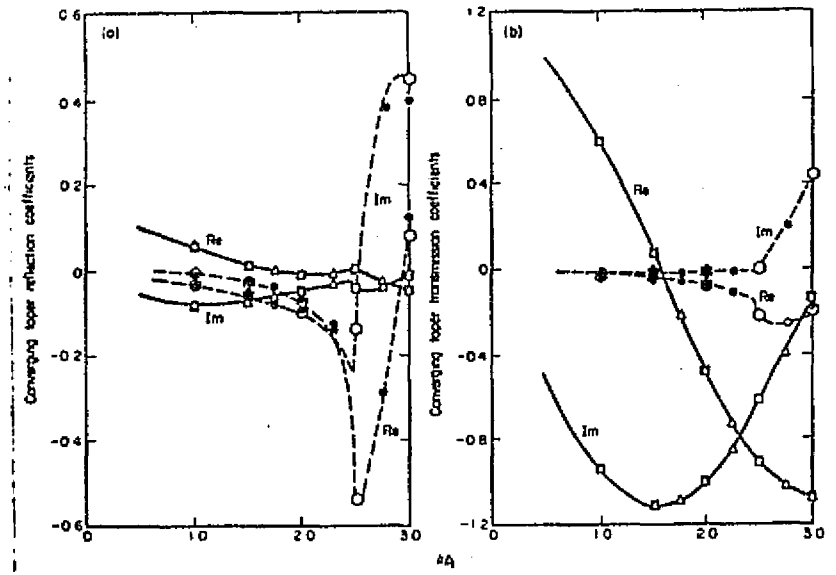

Figure 5. (a) Transmission coefficients and (b) reflection coefficients for modes 1 and 2 with mode 1 incident. Converging 15° linearly tapered unlined transition section. $kb_0 = 1{\cdot}27\ kb_1$. $\alpha = 15°$; $L = b_1$.

Mode 1	Mode 2	Method
——	-----	5 section stepped duct
△	●	Variational (Fourier bases)
□	○	Weighted residuals

eigenfunction expansion method and the MWR remain in close agreement but they do not agree closely with either stepped duct result at the higher kb_0. The imaginary part of the reflection coefficient is the first to show significant deviation. We have concluded that our choice of the number of modes in the stepped duct approximation was not adequate at the higher frequency, particularly after the second mode begins to cut on.

Figures 5(a) and (b) combine the results for transmission and reflection coefficients in the first and second modes with mode 1 incident for the converging taper. In this case the 5 section stepped duct and the variational method are used for comparison. Agreement is good throughout the frequency range. The stepped duct approximation appears to be more adequate in this case than in the diverging case, particularly for reflection coefficients, since more modes are used on the reflection side than were used in the diverging duct case.

As a second comparison we have analyzed at selected frequencies the transmission and reflection characteristics of a lined diverging transition section between uniform hard-wall ducts. We have used a cosine shaped transition which has the same small and large heights and the same length as the linear taper previously discussed. The only available results for comparison are from the variational approach. We encountered convergence problems with the variational scheme as our limited computational capacity permitted neither double precision nor more than 40 input basis functions. A series of results were obtained for which 4 axial cosine waves, 4 axial sine waves and from 5 to 9 transverse functions were used. In all cases convergence was observed to be occurring with increasing modes, but in several cases it was not reached to our satisfaction (judged by comparing successive runs with more and more

modes). For this reason we have only made comparisons where convergence in the variational case was acceptable. The MWR was used with 6 transverse modes and 50 axial integration steps. We have generated results in the form of reflection and transmission coefficients in modes 1 through 3 for mode 1 incident. Results are compared in Table 1. Absence of variational results indicates a lack of convergence at the level of approximation used. Wherever converged results are available, the MWR shows acceptable agreement with the variational approach. Because of the computer limitations noted in the variational results, the MWR results are considered the more accurate.

TABLE 1

Reflection and transmission coefficients for a cosine shaped lined transition section. First mode incident; amplitude = 1·0 + 0·0i

	Method of weighted residuals		Variational method	
kb_0	Reflection in first three modes	Transmission in first three modes	Reflection in first three modes	Transmission in first three modes
1·5	−0·05 + 0·27i	−0·18 − 0·61i	−0·03 + 0·28i	−0·17 − 0·61i
	−0·00 + 0·14i	0·17 + 0·20i	0·01 + 0·13i	0·18 + 0·20i
	0·01 − 0·03i	−0·04 − 0·03i		−0·04 − 0·04i
2·0	0·15 + 0·08i	−0·26 − 0·40i	0·17 + 0·06i	−0·25 − 0·41i
	0·15 + 0·21i	0·54 + 0·02i	0·16 + 0·17i	0·55 − 0·00i
	−0·01 − 0·05i	−0·08 + 0·03i		−0·10 + 0·02i
2·5	−0·11 − 0·02i	−0·47 − 0·44i	−0·11 − 0·02i	−0·48 − 0·44i
	0·19 − 0·02i	0·23 − 1·02i		0·19 − 1·02i
	−0·02 − 0·04i	0·01 + 0·08i	−0·02 − 0·03i	0·01 + 0·10i
3·0	−0·03 + 0·04i	−0·67 − 0·14i	−0·03 + 0·04i	−0·67 − 0·13i
	0·25 − 0·03i	−0·41 − 0·58i	0·19 − 0·05i	−0·42 − 0·55i
	−0·02 − 0·04i	0·02 + 0·05i	−0·02 − 0·03i	0·02 + 0·06i

Note: at each reduced frequency the first two columns are the converged result from MWR. The second two columns are from the variational method when a converged result is available.

$kb_0 = 1{\cdot}5$, $A = 0{\cdot}413 + 0{\cdot}720i$ $\quad kb_0 = 2{\cdot}5$, $A = 0{\cdot}788 + 0{\cdot}536i$

$kb_0 = 2{\cdot}0$, $A = 0{\cdot}664 + 0{\cdot}720i$ $\quad kb_0 = 3{\cdot}0$, $A = 0{\cdot}760 + 0\ 300i$

The results with which we have compared are all at relatively low frequency at which at most two modes propagate. We do not currently have available higher frequency results against which to compare, principally due to limitations in the computer facilities which we have used. However, we can gain a measure of confidence in the MWR by investigating its convergence properties at higher frequencies. We have considered the cosine shaped diverging transition section at a reduced frequency of $kb_0 = 12{\cdot}57$ and for a lining with $A = 0{\cdot}76 + 0{\cdot}30i$. In this case in the small duct the plane wave and 3 higher modes are well cut on and mode 5 is just cutting on. In the large duct the plane wave and 5 higher modes propagate ($kb_1 = 15{\cdot}94$). We have used four combinations of basis functions and integration steps beginning with 6 transverse modes and 50 steps and progressing through 8 modes and 50 steps, 6 modes and 100 steps, and 10 modes and 50 steps. Increasing the number of integration steps made virtually no difference. Increasing the number of basis functions provided a very definite convergence trend. To illustrate this convergence of the method we have shown in Table 2 the reflection coefficients in mode 5 due to all incident modes (REF_{5i}). Mode 5 was chosen because the driving reduced frequency is right at the mode 5 cut-on frequency in the source-side duct. This causes relatively large reflected components in this mode for any incident mode. In addition, in Table 2 we have shown the direct transmission coefficients in all incident

TABLE 2

Convergence trends in cosine shaped diverging transition.

$kb_0 = 12{\cdot}57$, $A = 0{\cdot}76 + 0{\cdot}31i$, $b_0 = 1{\cdot}0$, $b_1 = 1{\cdot}268$, $L = 1{\cdot}0$

Incident mode	Reflection coefficients in mode 5			Direct transmission coefficients		
	6 Basis FNS	8 Basis FNS	10 Basis FNS	6 Basis FNS	8 Basis FNS	10 Basis FNS
1	−0·223	−0·215	−0·2122	0·736	0·736	0·736
	+0·152i	+0·141i	+0·138i	+0·034i	+0·034i	+0·034i
2	0·230	0·222	0·2186	0·523	0·523	0·522
	−0·151i	−0·139i	−0·136i	+0·213i	+0·212i	+0·212i
3	−0·245	−0·232	−0·228	0·146	0·148	0·148
	+0·146i	+0·132i	+0·129i	+0·451i	+0·451i	+0·451i
4	0·260	0·238	0·232	−0·337	−0·341	−0·342
	−0·191i	−0·190i	−0·188i	+0·024i	+0·029i	+0·031i
5	−0·900	−0·896	−0·896	0·016	0·017	0·018
	+0·080i	+0·080i	+0·080i	+0·012i	+0·012i	+0·012i
6	0·279	0·272	0·269	−0·057	−0·060	−0·061
	+0·152i	+0·161i	+0·164i	−0·012i	−0·016i	−0·017i
7		−0·194	−0·191		−0·005	−0·005
		−0·128i	−0·130i		+0·002i	+0·002i
8		0·157	0·154		−0·002	−0·002
		+0·108i	+0·111i		+0·002i	+0·001i
9			−0·130			−0·001
			−0·097i			+0·001i
10			0·114			−0·000
			+0·087i			+0·001i

modes ($TRAN_{ii}$). Coefficients are shown for 6, 8 and 10 basis functions. The sequence of results is distinctly convergent. In this case the use of 8 basis functions is probably sufficient from an engineering standpoint.

As a final example of the use of the method we have computed the acoustic power balance for the linear converging taper between uniform hardwall ducts in the case when the taper is

TABLE 3

Acoustic power balance in linear taper converging transition section.

$kb_0 = 15{\cdot}94$, $b_0 = 1{\cdot}268$, $b_1 = 1{\cdot}0$, $L = 1{\cdot}0$

Incident mode	Incident power	Reflected power	Transmitted power	Absorbed power
$A = 0{\cdot}76 + 0{\cdot}30i$				
1	1·000	0·003	0·754	0·242
2	1·000	0·007	0·595	0·399
3	1·000	0·010	0·672	0·317
4	1·000	0·015	0·571	0·414
5	1·000	0·020	0·307	0·674
6	1·000	0·169	0·050	0·781
$A = 0{\cdot}0001 + 0{\cdot}0001i$				
1	1·000	0·004	0·996	0·000
2	1·000	0·0075	0·9923	0·000
3	1·000	0·026	0·974	0·000
4	1·000	0·148	0·852	0·000
5	1·000	0·557	0·443	0·000
6	1·000	0·948	0·052	0·000

lined ($A = 0{\cdot}76 + 0{\cdot}30i$) and also in the hard-wall case at $kb_0 = 15{\cdot}94$. For each propagating mode incident on the non-uniformity we have computed the incident power, the reflected power, and the transmitted power carried in all resulting propagating modes. The power dissipated in the acoustic lining is the amount by which the sum of the reflected and transmitted powers fail to match the incident power. Table 3 shows the results of these computations for both cases. The hard-wall case ($A = 0{\cdot}0001 + 0{\cdot}0001i$) is significant in that it adequately approximates the known result that no power is dissipated in the non-uniformity. While we have not at this point made extensive parametric variations, it appears from these results that the reflective characteristics of a non-uniformity can be enhanced for modes near the cut-off condition. We intend to report more detailed investigations of specific non-uniformities at a later date.

5. DISCUSSION AND CONCLUSIONS

The method of weighted residuals has been shown to be an accurate and rapidly convergent method for the computation of the acoustic transmission and reflection properties of non-uniformities in ducts without flow. Other methods applicable to the problem have been implemented and numerous comparison runs have been made to validate the MWR and to build confidence in its use. In all cases where other results could be generated, comparable results were obtained. As with any numerical technique, care must be exercised in the use of MWR. The choice of basis functions appears to favor good convergence characteristics, but in any new physical situation convergence experimentation should be undertaken.

One of the reviewers of the original version of this paper offered the suggestion that basis functions which satisfy

$$\psi'' + \kappa^2\psi = 0,\ \psi'(0) = 0 \qquad \text{and} \qquad \psi'(b) = -\frac{ikbA}{\cos\theta}\psi(b)$$

be considered. This is equivalent to using an effective admittance $A^* = A/\cos\theta$. If this is done the eigenvalue equation is

$$\kappa b \tan \kappa b = \frac{ikbA}{\cos\theta}. \tag{35}$$

The array of coupling coefficients, U^p_{mn}, then vanishes. While this is attractive it should also be noted that this would complicate the computation of $d\kappa_n/dx$, and hence U^a_{mn} and P^a_{mn}, and effectively introduce more coupling there. Hence, whether this is really a better set of basis functions would require numerical experimentation. The important point to be made is that the optimum use of methods of this type depends on extension experience in the particular application.

It has also been pointed out that the differential equation for the eigenvalues, equation (34), becomes singular when the impedance assumes the Cremer optimum value [2]. This is because the optimum is defined by a double eigenvalue and, as Zorumski [24] points out, a double eigenvalue implies that not only is

$$\kappa_n b \tan \kappa_n b = ikbA$$

but also

$$\frac{d}{d\kappa_n b}[\kappa_n b \tan \kappa_n b - ikbA] = 0.$$

This means that

$$2\kappa_n b + \sin 2\kappa_n b = 0$$

at a double point. When this occurs it is apparent that equation (34) is singular. Of course this problem is not unique to this method. The Newton-Raphson iteration would display a similar problem in computing eigenvalues as a function of some changing parameter if the double point were encountered. If this occurs and if it cannot be circumvented by testing for the occurrence and employing an expansion of the differential equation at the singular point to get past it, then a different set of eigenfunctions might be employed. For example, those generated from equation (35) would not have the same double points as ones generated from equation (33).

Our philosophy has been that with improved analysis methods for finite, non-uniform ducts with multi-modal propagation, the practical importance of the Cremer optimum has been reduced in that the optimum lining will generally not correspond exactly to the double point. We view the potential difficulty as important but not crucial to the utility of the method.

The non-uniformities treated in this paper are of the type which one might encounter in applications. They are not small, nor are they very abrupt (although all of the results for lined ducts presented here have a discontinuous change from hard-wall to soft-wall). It is to be expected that the more radical the non-uniformity, the less rapid will be the convergence, and the more basis functions and integration intervals will be required to achieve a satisfactory result. This is an inherent property of this type of method. At this point we are satisfied that we can treat problems of practical importance.

The results to date conclusively show that it is important to treat the duct non-uniformity problem from a multi-modal standpoint. A given incident mode will generate spurious reflected and transmitted modes which can have an important effect on acoustic lining design and radiation properties. In addition there appears to be a possibility of using geometry changes and their attendant reflective properties to enhance acoustic attenuation, but the multi-modal performance of the duct will have to be known for design purposes.

The problem of the most immediate importance is the extension of the method to the case of ducts with flow. In contrast to other methods investigated, the MSR appears to be extendable when flow is involved. Of course the complexity of the problem expands considerably, but the basic numerical scheme can be modified and expanded to include this case. Our research program is currently directed toward achieving a workable method when flow is present.

After the original version of this paper was written an expanded version of the work of Zorumski and Clark [6] has appeared as a NASA document [25]. The work in this document is quite appropriate to the development of the interface relations of equations (24a) and (24b) and is closely related to the development of equations (25) and (26).

ACKNOWLEDGMENT

The work described here was supported by the NASA Lewis Research Center under a grant to Wichita State University.

REFERENCES

1. P. M. Morse 1939 *Journal of the Acoustical Society of America* 11, 205–210. The transmission of sound inside pipes.
2. L. Cremer 1953 *Acustica* 3, 249–263. Theorie der luftschalldampfung in rechtekkanal mit schluckender wand und das sich dabei ergebende hochste dampfungsmass.

3. P. Munger and G. M. L. Gladwell 1969 *Journal of Sound and Vibration* 9, 28–48. Acoustic wave propagation in a sheared fluid contained in a duct.
4. W. Eversman 1970 *Journal of the Acoustical Society of America* 48, 425–428. The effect of Mach number on the tuning of an acoustic lining in a flow duct.
5. W. Eversman 1971 *Journal of the Acoustical Society of America* 49, 1372–1380 Effect of boundary layer on the transmission and attenuation of sound in an acoustically treated circular duct.
6. W. E. Zorumski and L. R. Clark 1971 *NASA Langley Research Center, Unpublished Working Paper.* Sound radiation from a source in an acoustically treated circular duct.
7. R. J. Alfredson 1972 *Journal of Sound and Vibration* 23, 433–442. The propagation of sound in a circular duct of continuously varying cross-sectional area.
8. E. Bahar 1967 *Radio Science* 2, 287–297. Generalized scattering matrix equations for waveguide structures of varying surface impedance boundaries.
9. R. J. Beckemeyer and W. Eversman 1973 *Proceedings of the American Institute of Aeronautics and Astronautics Aero-Acoustics Conference, Seattle, Washington, October* 15–17, *Paper* 73–1006. Computational methods for studying acoustic propagation in non-uniform waveguides.
10. A. H. Nayfeh, D. P. Telionis and S. G. Lekoudis 1973 *Proceedings of the American Institute of Aeronautics and Astronautics Aero-Acoustics Conference, Seattle, Washington, October* 15–17, *Paper* 73–1008. Acoustic propagation in ducts with varying cross sections and sheared mean flow.
11. L. S. King and K. Karamcheti 1973 *Proceedings of the American Institute of Aeronautics and Astronautics Aero-Acoustics Conference, Seattle, Washington, October* 15–17, *Paper* 73–1009. Propagation of plane waves in the flow through a variable area duct.
12. P. Huerre and K. Karamcheti 1973 *Proceedings of Interagency Symposium on University Research in Transportation Noise, Stanford University, March* 28–30. Propagation of sound through a fluid moving in a duct of varying area.
13. A. Powell 1960 *Journal of the Acoustical Society of America* 32, 1640–1646. Theory of sound propagation through ducts carrying high speed flow.
14. N. A. Eisenberg and T. W. Kao 1960 *Journal of the Acoustical Society of America* 49, 169–175. Propagation of sound through a variable area duct with a steady compressible flow.
15. C. K. W. Tam 1971 *Journal of Sound and Vibration* 18, 339–351. Transmission of spinning acoustic modes in a slightly non-uniform duct.
16. A. Cummings 1973 *Journal of Sound and Vibration* 31, 331–343. Acoustics of a wine bottle.
17. S. A. Schelkunoff 1952 *Bell System Technical Journal* 31, 784–801. Generalized telegraphist's equations for waveguides.
18. S. A. Schelkunoff 1955 *Bell System Technical Journal* 39, 955–1043. Conversion of Maxwell's equations into generalized telegraphist's equations.
19. A. F. Stevenson 1951 *Journal of Applied Physics* 22, 1447–1460. General theory of electromagnetic horns.
20. A. F. Stevenson 1951 *Journal of Applied Physics* 22, 1461–1463. Exact and approximate equations for wave propagation in acoustic horns.
21. G. Reiter 1959 *Proceedings of the Institution of Electrical Engineers* 106, Part B, Supplement 13, 54–57. Generalized telegraphist's equations for waveguides of varying cross section.
22. B. A. Finlayson 1972. *The Method of Weighted Residuals and Variational Principles.* Academic Press.
23. D. L. Lansing and W. E. Zorumski 1973 *Journal of Sound and Vibration* 27, 85–100. Effects of wall admittance changes on duct transmission and radiation of sound.
24. W. E. Zorumski and J. P. Mason 1974 *Journal of the Acoustical Society of America.* Multiple eigenvalues of sound absorbing circular and annular ducts.
25. W. E. Zorumski 1974 *NASA TR*-419. Acoustic theory of axisymmetric multisectioned ducts.

Appendix B

REPRODUCTION OF PAPER DESCRIBING EIGNEVALUE ROUTINE

MS079

Journal of Sound and Vibration (1975) 40(4), ;;;–;;;

COMPUTATION OF AXIAL AND TRANSVERSE WAVE NUMBERS FOR UNIFORM TWO-DIMENSIONAL DUCTS WITH FLOW USING A NUMERICAL INTEGRATION SCHEME

1. INTRODUCTION

The purpose of this letter is to detail a scheme by which the axial and transverse wave numbers for propagation of sound in uniform two-dimensional ducts with uniform flow can be computed. In the method used the eigenvalue equation is transformed into a first order non-linear ordinary differential equation. By using appropriate initial values this differential equation is integrated by using a Runge-Kutta algorithm to yield solutions which are the transverse wave numbers for the duct. The transverse wave numbers then are used to compute the axial wave numbers. The method proposed is particularly useful for the rapid computation of a number of duct eigenvalues at a single reduced frequency, lining admittance and duct flow Mach number. It has the advantage of being an inherently stable computational scheme. In addition, the ordering of the eigenvalues is well defined by their relationship to a corresponding set of hard-wall eigenvalues (the initial values in the integration scheme).

2. METHOD

The specific problem is that of propagation of sound in a uniform two-dimensional duct of height b with one wall hard and the other with a lining admittance A. This configuration can be viewed as modelling a duct with this lining arrangement or a duct of height $2b$, symmetrically lined, with symmetric propagation. Propagation at reduced frequency kb is considered, where k is the plane wave wave number $k = \omega/c$, ω being the driving frequency and c the speed of sound. The duct Mach number, M, is assumed to be subsonic.

It is well known that for this situation propagation in the duct can be represented by a superposition of acoustic modes of the form

$$p_n = A_n e^{i\omega t} e^{-ik_{x_n} x} \cos \kappa_n y,$$

where x is the duct axial co-ordinate and y is the transverse co-ordinate measured from the hard wall. κ_n is the transverse wave number for the nth mode of propagation and k_{x_n} is the corresponding axial wave number. They are defined by the simultaneous eigenvalue equations

$$kb\left(\frac{\kappa}{k}\right)\tan kb\left(\frac{\kappa}{k}\right) = iAkb\left(1 - M\frac{k_x}{k}\right)^2, \tag{1}$$

$$\frac{k_x}{k} = \frac{1}{1-M^2}\left(-M \pm \left[1-(1-M^2)\left(\frac{\kappa}{k}\right)^2\right]^{1/2}\right). \tag{2}$$

For the present analysis equations (1) and (2) are considered in the somewhat modified form

$$kb\left(\frac{\kappa}{k}\right)\tan kb\left(\frac{\kappa}{k}\right) = iAkbw^2, \tag{3}$$

$$w = \frac{1 \mp M\left[1-(1-M^2)\left(\frac{\kappa}{k}\right)^2\right]^{1/2}}{1-M^2}. \tag{4}$$

Throughout the analysis it is important to maintain consistency in the ± sign choice. The significance of the sign choice is straightforward for ducts with attenuation. In this case the axial wave number is written as

$$k_x/k = \alpha \pm i\beta,$$

$$\beta = Im\left[1-(1-M^2)\left(\frac{\kappa}{k}\right)^2\right]^{1/2},$$

and the square root is the principal value taken in the upper half plane (positive imaginary part). The modes of propagation are in the form

$$p_n = A_n e^{i(\omega t - \kappa_n x)} e^{\mp \beta_n x} \cos \kappa_n y.$$

In order to have attenuation with increasing x it is necessary to choose the negative sign in equation (2) or equation (4). Acoustic modes defined according to this convention will correspond to propagation in the positive x direction. If the flow is taken to be in the positive x direction, then this will represent propagation with the flow (exhaust mode). When the positive sign is chosen in equation (2) or equation (4) one defines propagation in the negative x direction, against the flow (inlet mode). In the case when β is identically zero, which occurs when $\kappa/k = 0$ or κ/k is real and $1-(1-M^2)(\kappa/k)^2 > 0$, the principal value of the square root is taken on the regative real axis. (This is done so that the sign choices given above always relate the same way to right and left running waves.)

The usual way to obtain selected eigenvalues of the doubly infinite sequence of κ_n and k_{x_n} defined by equations (1) and (2) or equations (3) and (4) consists of using an iteration scheme based on suitable initial guesses. Users of this method are well aware of potential instabilities, difficulties encountered in ordering the results, and the requirement for accurate initial guesses. Successful numerical schemes based on the iteration approach are in existence but generally have to be quite sophisticated to overcome the problems indicated. The method that introduced here is both simple and accurate.

One considers the eigenvalue κ_n/k to be a function of some parameter, η. In general, one also would consider kb, A and M to be functions of this parameter. If equations (3) and (4) are differentiated with respect to η and combined, then the following single ordinary differential equation results:

$$\left[\tan kb\left(\frac{\kappa}{k}\right) + kb\left(\frac{\kappa}{k}\right)\sec^2 kb\left(\frac{\kappa}{k}\right) \mp \frac{2iAw}{v^{1/2}} M\left(\frac{\kappa}{k}\right)\right]\frac{d}{d\eta}\left(\frac{\kappa}{k}\right)$$

$$= iw^2\frac{dA}{d\eta} - \left(\frac{\kappa}{k}\right)^2 \sec^2 kb\left(\frac{\kappa}{k}\right)\frac{d}{d\eta}(kb) \mp \frac{2iAw}{v^{1/2}(1-M^2)}\left[2w - 1 - \left(\frac{\kappa}{k}\right)^2\right]\frac{dM}{d\eta}, \tag{5}$$

where

$$v = 1-(1-M^2)\left(\frac{\kappa}{k}\right)^2$$

and $v^{1/2}$ is the principal value of the square root as defined previously.

If κ/k is known for some combination A, kb, M, then equation (5) is a differential equation defining the variation of κ/k as A, kb, m change as functions of η from the original values.

Equation (5) can be used in two different ways. In the simplest application, and the one which is the major subject of this paper, one considers kb and M to be independent of η. Then the differential equation describes the variation of κ/k as A varies with η. Hence, if A is given some prescribed variation, the corresponding variation in κ/k can be obtained by integration.

Consider the problem of finding the eigenvalues defined by equations (3) and (4) for a specific condition A, kb, M. If $A = 0$ the eigenvalues are known to be

$$\frac{\kappa_n}{k} = \frac{(n-1)\pi}{kb}, \quad n = 1, 2. \tag{6}$$

Now let A vary according to $A(\eta) = \eta A_f$, where $0 < \eta < 1$. Equation (5) becomes

$$\frac{d}{d\eta}\left(\frac{\kappa}{k}\right) = \frac{iw^2 A_f}{\left[\tan kb\left(\frac{\kappa}{k}\right) + kb\left(\frac{\kappa}{k}\right)\sec^2 kb\left(\frac{\kappa}{k}\right) \mp 2i\frac{Aw}{v^{1/2}} M\left(\frac{\kappa}{k}\right)\right]}. \tag{7}$$

If equation (7) is integrated on $0 < \eta < 1$, a hard-wall eigenvalue from the sequence of equation (6) being used as the initial value, then at $\eta = 1$ the solution to equation (7) will be an eigenvalue for the condition A_f, kb, M. Furthermore, it can be identified as the eigenvalue which branches from the hard-wall eigenvalue on the real axis in the κ/k plane which was used as an initial value. Each hard-wall eigenvalue on the real axis branches into two soft-wall eigenvalues, one for propagation in the positive x direction and the other for propagation in the negative x direction (corresponding to the sign choice). Hence, starting with N hardwall eigenvalues, one can compute $2N$ eigenvalues (n exhaust mode eigenvalues and N inlet mode eigenvalues) for the duct conditions A_f, kb, M simply by integration of equation (7) on $0 < \eta < 1$ with hard-wall eigenvalues as initial values. For each eigenvalue, κ/k, one can compute the corresponding axial wave number, k_x/k, by using equation (2).

A second application of equation (5) has proved useful in the study of non-uniform ducts; in this case A, kb, and M can be considered to be functions of the axial co-ordinate, x. In this case, equation (5) defines the variation of the eigenvalues, κ/k, with respect to axial position. The starting values in this case would be the eigenvalues corresponding to the conditions at the starting point, say $x = 0$. The eigenvalues at this starting point could be computed conveniently by using equation (7).

Yet a third application, not implemented as yet by the author, would provide a means of carrying out parametric variations to determine the variation in duct attenuation values with independent variations in A, kb or M. For example, if it were desired to compute the variation in attenuation for a given lining admittance at a given Mach number for variations in kb one could construct a simple functional dependence for kb, say

$$kb(\eta) = \eta(kb)_f,$$

$(kb)_f$ being the highest kb required. If the initial values are chosen as known eigenvalues when η takes on its initial value, η_0, and if the integration is carried out on $\eta_0 < \eta < 1$, then one rapidly can generate the results of the parametric variation.

3. IMPLEMENTATION

The computational scheme follows nearly exactly the theoretical development described above. A fourth order Runge–Kutta integration package has been used. In solving the basic eigenvalue problem as defined by equation (7), a variable step size has been used, starting with 2% of the full interval for the first five steps and then switching to 10% for the last nine steps. To possibly increase the accuracy of the results a Newton–Raphson interaction has

been used at the end of the integration for each eigenvalue to refine the result which may have some accumulated error due to the rather coarse integration grid. Experience to date shows very little need to do this. The best way to judge the error is to insert the computed eigenvalue at the current integration step into the eigenvalue equation, equation (3), and evaluate the residual developed. It has been found that if a significant residual develops it usually will be in the first step away from the initial value. It may prove worthwhile to use the developing residual to automatically vary the step size.

The only instance in which equation (7) or equation (5) requires special attention is when it becomes singular. This always occurs in using equation (7) when one steps away from the hard-wall eigenvalue, $\kappa/k = 0$. It also can arise when a double eigenvalue occurs. While the second situation is possible, no special precautions to account for it have been taken by the author, the philosophy being that the chance of it occurring is remote unless one is specifically attempting to compute the double eigenvalue. It is worth mentioning that the use of an automatically variable step size based on the current residual provides an excellent means of controlling the accuracy when the integration passes near a singular point.

When it is required to step away from the hard-wall eigenvalue, $\kappa/k = 0$, in equation (7), the first step is made by noting that for small A and small κ/k one can write

$$\frac{\kappa}{k} \simeq \frac{ikb\Delta A_f}{1 - M^2}(1 \pm M),$$

where Δ is the initial step away from $\eta = 0$ which in the author's implementation has been 2% of the total interval. This result is then refined, by using a Newton–Raphson scheme, and used as a starting value for an integration beginning at $\eta = 0{\cdot}02$.

Department of Mechanical Engineering,
University of Canterbury,
Christchurch 1, New Zealand
W. EVERSMAN

(*Received 4 March* 1975)